**POLITECNICO DI MILANO**

**Master of Science in Automation Engineering**

**Department of Electronics, Information and Bioengineering**


# Distributed cerebellar plasticity implements generalized multiple-scale memory components in real-robot sensorimotor tasks

**NearLab**

**Neuro Engineering and medical Robotics Laboratory**

**Supervisor: Prof. Alessandra Laura Giulia Pedrocchi**

**Co-Supervisor: Dr. Claudia Casellato**

**Author: Ladan Emamjomeh**

Academic year 2013/2014

# Table of Contents

# Abstract

The cerebellum plays a crucial role in motor learning and it acts as a predictive controller. Modeling it and embedding it into sensorimotor tasks allows us to create functional links between plasticity mechanisms, neural circuits and behavioral learning. Moreover, if applied to real-time control of a Neurorobot, the cerebellar model has to deal with a real noisy and changing environment, thus showing its robustness and effectiveness in learning.

A biologically inspired cerebellar model with distributed plasticity, both at cortical and nuclear sites, has been used. Two cerebellum-mediated paradigms have been designed: an associative Pavlovian task and a vestibulo-ocular reflex, with multiple sessions of acquisition and extinction and with different stimuli/perturbation patterns. The cerebellar controller succeeded to generate conditioned responses and finely tuned eye movement compensation, thus reproducing human-like behavior. Through a productive plasticity transfer from cortical to nuclear sites, the 3-site distributed cerebellar controller showed in both tasks the capability to optimize the learning on multiple time-scales, to store permanent motor memory and to effectively adapt to dynamic ranges of stimuli.

In the dissertation the following steps have been carried out:

- Design of Robotic protocols
- Controller development embedding the cerebellum adaptive model
- Test and results interpretation

# Sommario

Il cervelletto svolge un ruolo cruciale nell'apprendimento motorio ed agisce come un controllore predittivo. La sua modellazione e integrazione all'interno di compiti sensorimotori permette di creare legami funzionali tra i meccanismi di plasticità, i circuiti neurali e l'apprendimento comportamentale. Inoltre, se applicato al controllo in tempo reale di un Neurorobot, il modello cerebellare deve svolgere il suo compito all'interno di un ambiente rumoroso e variabile, dimostrando in questo modo la sua robustezza ed efficacia nel processo di apprendimento.

In questo lavoro è stato utilizzato un modello biologicamente ispirato al cervelletto, con una plasticità distribuita sia a livello corticale sia a livello dei nuclei cerebellari profondi. Sono stati progettati due paradigmi di apprendimento nei quali il cervelletto svolge un ruolo predominante: un compito di associazione temporale pavloviana e il riflesso vestibolo-oculare. I paradigmi sviluppati prevedevano sessioni multiple di acquisizione ed estinzione e differenti tipologie di stimolo/perturbazione. Il controllore cerebellare è riuscito a generare risposte condizionate e a regolare in modo fine il movimento degli occhi in risposta ad una rotazione della testa, riuscendo quindi a riprodurre il comportamento riscontrato nei soggetti umani in letteratura. Attraverso un produttivo trasferimento di plasticità dai siti di plasticità corticali a quelli nucleari, il controllore cerebellare provvisto di tre siti di plasticità ha mostrato in entrambi i compiti la capacità di ottimizzare l'apprendimento su molteplici scale temporali, di sviluppare una memoria motoria persistente e di adattarsi efficacemente ad una gamma dinamica di stimoli.

Nella tesi sono state sviluppate le seguenti parti:

- Progettazione di protocolli robotici
- Sviluppo di un controllore includendo il modello adattivo di cervelletto
- Test e interpretazione dei risultati

## Acknowledgment

I owe sincere and earnest thanks to Professor Alessandra Laura Giulia Pedrocchi and Dr. Claudia Casellato, my magnificent supervisors whom I had the opportunity to work with them and this project would not have been completed without their kind support, noble ideas, guidance, and attention. I learned much more than I could imagine from them during the thesis work. I am thankful for the opportunity to be part of this project. Also, I would like to show my deep grateful to Alberto Antonietti because of his generous helps during thesis work. Additionally, I would like to add my great thanks to whom made this Master degree an absolutely great experience. Thank you Professor Paolo Rocco for sharing your theoretical and scientific knowledge with me and I am grateful for the opportunity to be part of this Master program. To all above, I am truly gratitude for my family in Iran who are always there for me. They gave me everything and supported me during my studies. My mother, my both sisters, Mina and Laleh; my brother, and brother-in-law, Amin and Babak, who gave me the opportunity to be independent and taught me to be hopeful.

# List of Figure

# 1. Introduction

There has recently been a renewal of interest in studying the mechanisms and structure of the brain, and modeling these structures to yield systems that learn. To distinguish these computational structures from their biological counterparts they are called artificial neural networks. Artificial neural networks can be thought of as a class of computational models for representing non-linear input-output mappings. Learning occurs by training with examples rather than explicit programming. These properties make neural networks very attractive for robot control. Control of robots requires the solution of the complex inverse kinematic and dynamic equations, which is a computationally intensive process. Also the parameters of a robot such as moments of inertia and joint friction cannot be determined precisely and obtaining meaningful model equations is difficult. Hence the idea of obtaining these relations based on measured input- output data is very appealing.

Neurorobotics is a science which is a combination of neuroscience, robotics, and artificial intelligence studies as well as technology to represent autonomous neural systems. Neural systems include brain-inspired algorithms such as "connection networks", "computational models of biological neural networks", in conjunction with real biological nervous systems make neural systems. It is possible to represent such kind of neural systems either in machines with mechanic or any other forms of physical actuation. This includes robots, prosthetic or wearable systems but also, at smaller scale, micro-machines and, at the larger scales, furniture and infrastructures [1].

At its core, neurorobotics is based on the idea that the brain is embodied and the body is embedded in the environment. Therefore, most neurorobotics are required to function in the real world, as opposed to a simulated environment (Fig.1).

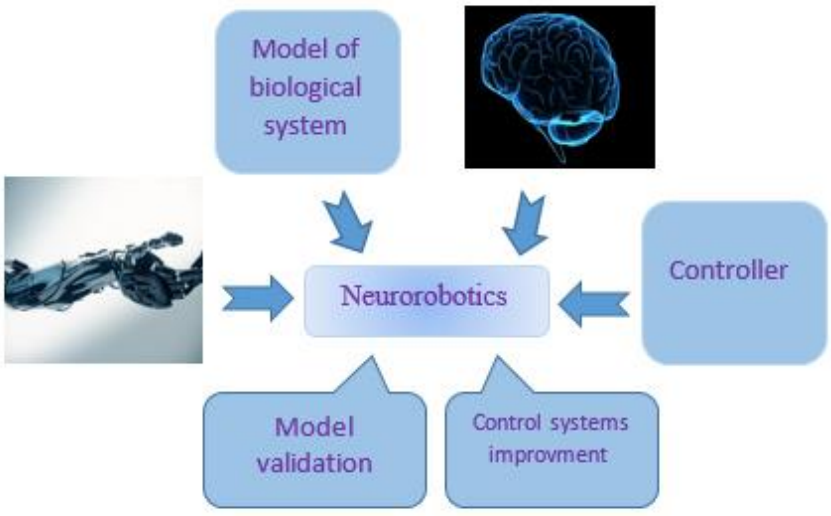


*Figure 1: Neurorobotics integrates brain-inspired modules and robotic devices and it allows to validate biological models or to improve the control system of robots*

The **Cerebellum** is a region of the brain that plays an important role in motor control [2]. Cerebellum-dependent learning is demonstrated in different contexts, such as multiple forms of associative learning, where the learning is based on the stimulus-response association. Eye-blink conditioning, saccadic eye movements, vestibular ocular reflex and reaching arm movements are well-known examples of these mechanisms.

The cerebellum does not initiate movement, but it contributes to coordination, precision, and accurate timing. It receives input from sensory systems of the spinal cord and from other parts of the brain, and integrates these inputs to fine tune motor activity. Cerebellar damage does not cause paralysis, but instead produces disorders in fine movement, equilibrium, posture, and motor learning.

What is the role of the cerebellum in the control of reaching movements? Bastian et al. (1996b) demonstrated that the cerebellum compensates for interaction torques that would otherwise push the arm off its desired equilibrium path during fast-reaching movements. While feedback control could, in principle, compensate for interaction torques, it is limited by both long delays in the nervous system and the dynamic properties of muscles and proprioceptors. The cerebellum can implement a Feed Forward, nonlinear predictive regulator by learning part of the inverse dynamics of the arm. After learning, accurate fast movements can be performed in spite of the long conduction delays [3].

The Vestibulo-ocular reflex is based on the temporal association of the two stimuli, head turn and motion of retinal image, i.e. the system learns that one stimulus will be followed by another stimulus and a consequent predictive compensatory response is gradually produced and accurately tuned.

Most of the theoretical models of the sensorimotor derive from early models formulated by David Marr and James Albus, which were motivated by the observation that each cerebellar Purkinje cell receives two dramatically different types of input: one type is of thousands of inputs from parallel fibers, each individually very weak; the other is the input from one single climbing fiber, which is, however, so strong that a single climbing fiber action potential will reliably cause a target Purkinje cell to fire a burst of action potentials. The basic concept of the Marr-Albus theory [4] is that the climbing fiber serves as a "teaching signal", which induces a long-lasting change in the strength of synchronously activated parallel fiber inputs. Observations of long-term depression in parallel fiber inputs have provided support for theories of this type, but their validity remains controversial.

Thus in order to learn and store information about body environment dynamics in internal models of movement so as to act as a predictive controller, the cerebellum is thought to employ long-term synaptic plasticity (Long-term Depression (LTD) and Long-Term Potentiation (LTP)). The plasticity at the Parallel Fibers/Purkinje Cells (PF-PC) synapses has classically been assumed to sub serve this function .

The aim of the project is the customization of a real human-like sensorimotor platform controlled by a cerebellum realistic model. It controls the robot through torque values which represent motor commands to its joints. Motor commands are added to an AD-HOC tuned feedback controller.

# 2. State of the Art

Motor learning result from practice or a novel experience, in the capability for responding in a complicated environment. It often involves improving the smoothness and accuracy of movements and is obviously necessary for complicated movements such as speaking, playing the piano, and climbing trees; but it is also important for calibrating simple movements like reflexes or associative patterns, as parameters of the body and environment change over time.

In the structure of motor control, human-like movement planning and adaptive neural systems inside the same controller can be a useful way for creating a control system that display a human-like behavior.

In the role of the cerebellum in motor control, it can say that is necessary for several types of motor learning, most notably learning to adjust to changes in sensorimotor relationships. Several theoretical models have been developed to explain sensorimotor calibration in terms of synaptic plasticity within the cerebellum.

In the following, we explain about the motor control and motor planning in detail and about the mechanisms of the learning in the cerebellum and the mechanisms of the controller in the robotic system.

## 2.1 Motor control and Motor Planning

Computational models can provide useful guidance in the design of behavioral and neurophysiological experiments and in the interpretation of complex, high dimensional biological data. Because many problems faced by the primate brain in the control of movement have parallels in robotic motor control, models and algorithms from robotics research provide useful inspiration, baseline performance, and sometimes direct analogs for neuroscience.

The theory of motor control was largely developed in classical engineering fields such as cybernetics, optimal control, and control theory [5].

The control diagram joining between computational modeling and theories in artificial intelligence and robotics in Figure 2 can also function as an abstract guideline for research in biological motor control. This diagram distinguishes between five major stages of motor control: first, the higher level processing and decision making, which defines the intent of the motor system; second, the motor planning stage; third, the potential need and problem of coordinate transformations; fourth, the final conversion of plans to motor commands; and fifth, the preprocessing of sensory information such that it is suitable for control. Of course, the separation of the stages in Figure 2 might not be present in some control algorithms and in biological systems, but, as will be seen below, a conceptual differentiation of these stages will be useful for our discussion [6].

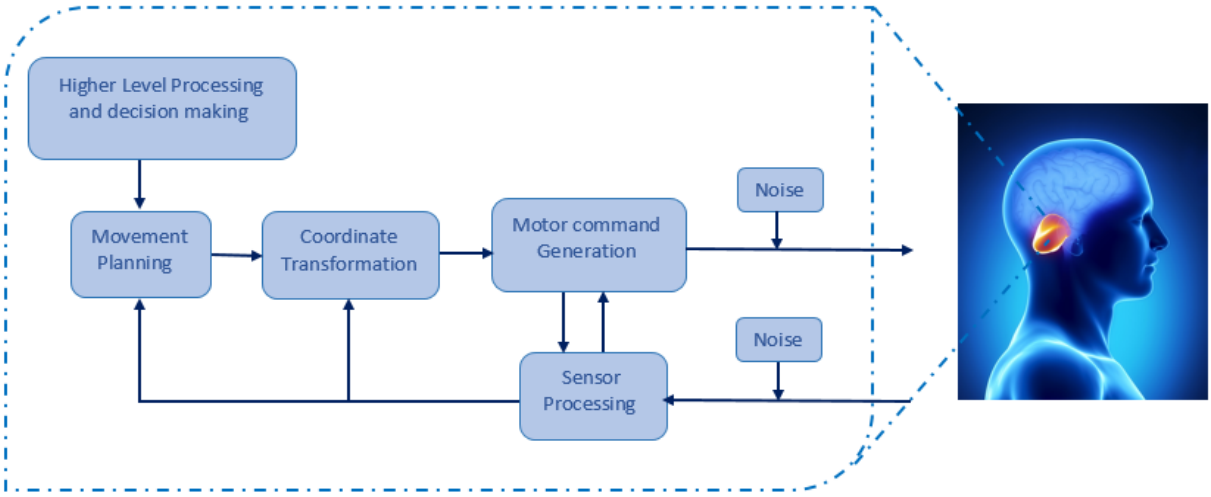


*Figure 2: Sketch of a generic motor control diagram, typically used in robotics research that can also function as a discussion guideline for biological motor control.*

The study of motor control is a fundamental of the study of sensorimotor transformations. For the motor control system to move its effectors to apply forces on objects in the world or to place its sensors with respect to objects in the world, it must coordinate a variety of forms of sensory and motor data. These data are generally in different formats and may refer to the same entities but in different coordinate systems. Transformations between these coordinate systems allow motor and sensory data to be related, closing the sensorimotor loop. Equally fundamental is the fact that the motor control system operates with dynamical systems, whose behavior depends on the way energy is stored and transformed. The study of motor control is therefore also the study of dynamics.

If we consider a sensorimotor loop, the coordinate transformations allow motor and sensory data to be related and they can be subdivided into kinematic and dynamic transformations. The kinematic transformations convert the systems coordinates (i.e. from Cartesian to joint coordinates) while dynamic transformations translate the coordinates in motor command (i.e. the force to apply in order to obtain the desired movement). Therefore the movements happen through three transformation: planning, inverse kinematic and inverse dynamic.

Redundant degrees of freedom is one of the problem of the moving organ (e.g. to move manipulator to a target position, there is an infinite number of possible paths that the manipulator could follow and for each of these paths there is an infinite number of velocity profiles the manipulator could follow) and motor planning is needed.

To solve the three levels of uncertainty of the system in motor control (i.e. kinematic chain, angular configurations and muscular activations) motor planning is a fundamental phase that is needed [7]. For any reach target there is infinite number of possible path and velocity pattern that a part of body or limb can follow. Once these parameters have been fixed, there are infinite combinations of muscle activations and infinite relative joint angle configurations that can achieve the established trajectory. Motor planning is thus the computational process that selects one single solution from the many alternatives provided for this task.

Indeed, with the motor planning we want to assign the way the robot evolves from an initial posture to a final one. Kinematic and dynamic models. A widely used kinematic based model is the minimum jerk model which predicts that the parameter controlled by the nervous system is the spatial path of the hand [8, 9].

On the other hand, the kinematic models give the positions and velocities of the arm joints so after continue planning, an inverse kinematic model is implemented to obtain joint-space kinematics.

Cerebellum plays a crucial role in motor coordination, following the organism to learn through trial and error what exact pattern and sequence of motor commands is necessary to produce rapid, accurate, and effortless movements.

We will review models that are aimed at understanding the cerebellum's possible role in motor learning and control at the functional level. The approaches we will review are intimately linked to the notion that the cerebellum contains an internal model or models of the motor apparatus. There are two varieties of internal model, forward and inverse models.

Forward models capture the forward or causal relationship between inputs to the system, such as the arm, and the outputs. A forward dynamic model of the arm, for example, predicts the next state (e.g. position and velocity) given the current state and the motor command. In contrast, inverse models invert the system by providing the motor command that will cause a desired change in state. They are, therefore, well suited to act as controllers as they can provide the motor command necessary to achieve some desired state transition.

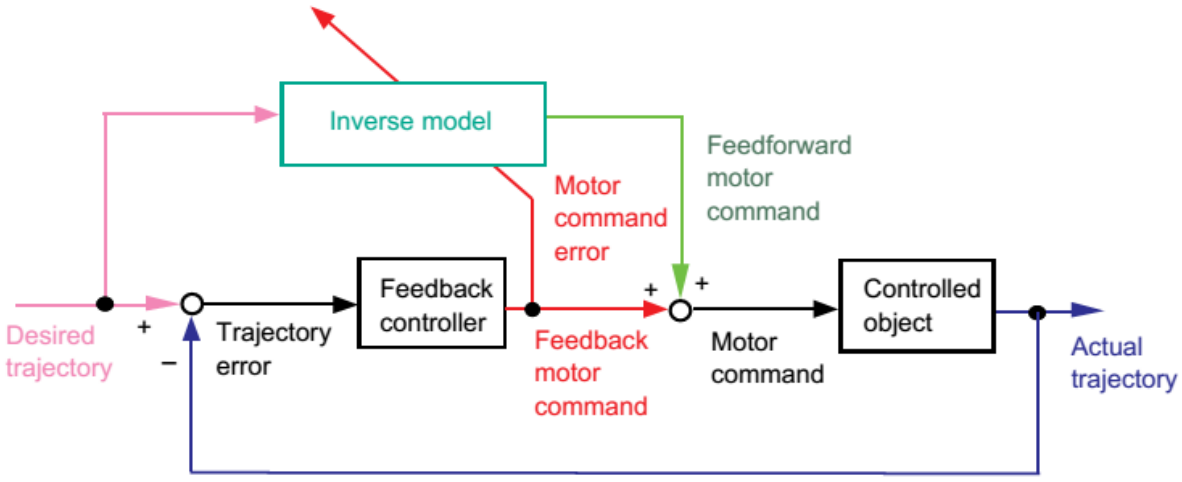


*Figure 3: The general feedback-error-learning model*

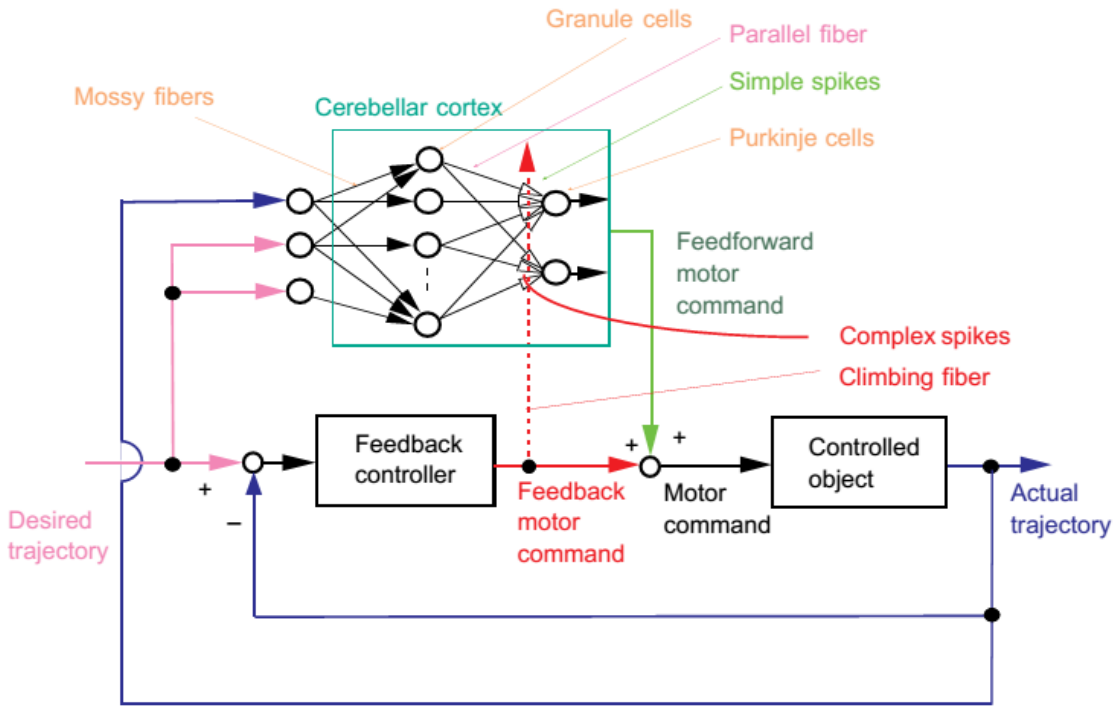


*Figure 4: The cerebellar feedback-error-learning model*

The 'controlled object' is a physical entity that needs to be controlled by the central nervous system (CNS), such as the eyes, hands, legs or torso [10]. The control system can be considered as a cascade of transformations between motor command (e.g. joint torques or muscle activations) and linkage motion (e.g. joint angular position, velocity and acceleration), and between this linkage motion and the controlled object motion .

## 2.2 Learning Mechanisms and the cerebellum

The cerebellar cortex is often viewed as an array of perceptrons (Marr 1969; Albus 1971; Ito 1984). In this theory, the granule cells (GCs) - Purkinje cell (PC) synapses can be modified by climbing fiber (CF) inputs.

The input to the cerebellum is characterized by its divergence from the mossy fibers (MF) to the GCs (Ito 1984). The GCs are known to give, via their axons, the parallel fibers, excitatory projections to the PCs and to all the inhibitory interneurons (basket, stellate and Golgi cells) of the cerebellar cortex. The Golgi cells (GOs) Feed-Back onto the GCs and have very powerful synapses with long lasting effects. As PCs have inhibitory action upon nuclear cells (collaterals of some MFs excite the nuclear cells), they modulate the signal flow from the nuclear cells. The PCs of the intermediate cerebellum project to the interpositus nucleus (IP), which itself projects to the motor cortex via the thalamus and to the spinal cord via the red nucleus.

Thus, the intermediate cerebellum plays a major role in controlling ongoing movements. The climbing fibers, which are the axons of inferior olive cells (IOs), convey signals encoding error in the

performance of the system in which the cerebellar subsystem is installed. CF signals induce long-term depression (LTD) in those PF-PC synapses that were activated in conjunction with the climbing fiber (Figure 5).

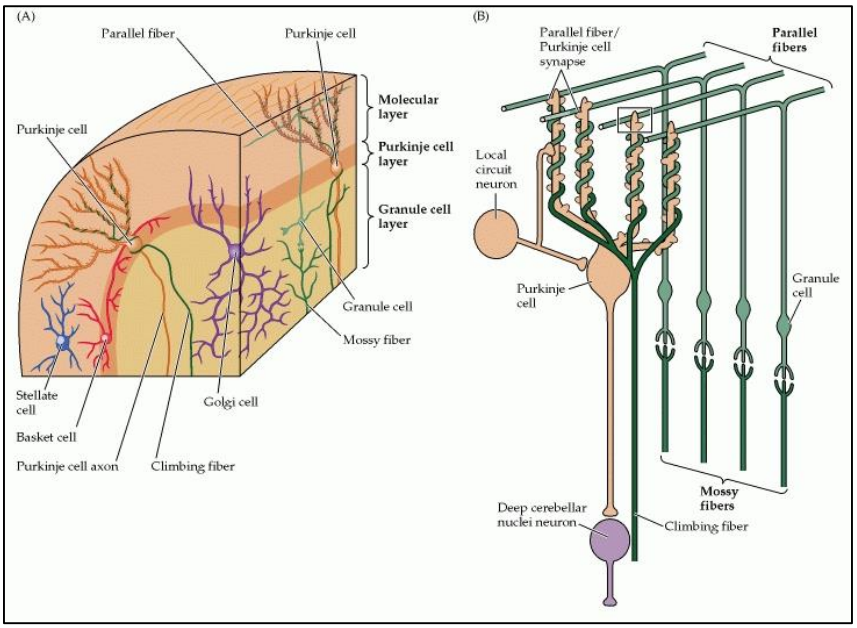


*Figure 5: The cerebellum microcircuit*

In order to learn and store information in internal models of movement so to act as a predictive controller, the cerebellum is thought to employ long-term synaptic plasticity (Long-Term Depression (LTD) and Long-Term Potentiation (LTP)). The plasticity at the Parallel Fibers/Purkinje Cells (PF-PC) synapses has classically been assumed to sub serve this function [4].

However, multiple processes, with different learning rates, may contribute to these mechanisms [11, 12,13] and PF-PC single plasticity cannot account for the broad dynamic ranges and multiple time scales of cerebellar adaptation. One hypothesis is that the cerebellum learns basically on two time scales ascribable to two anatomical sites: the cerebellar cortex operates as a fast learning module while deeper structures operate as a slow learning module where the motor skill is transferred and consolidated into more persistent memory [14]. Indeed, the activity of the Deep Cerebellar Nuclei (DCN) can be modulated; DCN spike times are strongly correlated with memory acquisition [15].However, there have been few physiological studies on long-term plasticity in DCN and on their roles in motor learning paradigms. Cerebellar cortical and nuclear plasticity have been proposed to be involved and complementary in controlling cerebellar learning in EyeBlink Classical Conditioning (EBCC) [16, 17, 18] and in Vestibulo-Ocular Reflex (VOR) [19, 20]. Indeed, inactivation of cerebellar cortex [21], cerebellar nuclei [22] or Inferior Olive (IO) [23] all prevent acquisition skills.

There are several possible molecular and cellular mechanisms that could underlie adaptation of the vestibulo-ocular reflex and Eyeblink conditioning. Behavioral observations showed common and robust mechanisms between EBCC and VOR tasks: slow and fast complementary adaptation

processes, spontaneous recovery of the original response and faster relearning through consolidation mechanisms. However, causal relationships between particular cellular processes individual components of a learned behavior have not been demonstrated unequivocally [24].

## 2.3 Control Mechanisms of Robotic Systems

### 2.3.1 Kinematic Model

Robot kinematics applies geometry to the study of the movement of multi-degree of freedom kinematic chains that form the structure of robotic systems. The emphasis on geometry means that the links of the robot are modeled as rigid bodies and its joints are assumed to provide pure rotation or translation.

Robot kinematics studies the relationship between the dimensions and connectivity of kinematic chains and the position, velocity and acceleration of each of the links in the robotic system, in order to plan and control movement and to compute actuator forces and torques.

The kinematic model is fundamental for motion planning and it is composed by two main components: the forward (direct) kinematic and the inverse kinematic.

The forward kinematic problem establishes the relationship between Cartesian coordinates (workspace) of the end effector and the joint angles in joint-space frame, once the joint position (q), velocity ($\dot{q}$) or acceleration ($\ddot{q}$) are known. It is embedded in a function f defined between the joint space ($\mathbb{R}^n$) and the work space ($\mathbb{R}^m$) such that:

$$x = f(q, \dot{q}, \ddot{q},), \qquad x \in \mathbb{R}^m \ , q \in \mathbb{R}^n$$

The inverse kinematic problem computes the joint angles as a function of the end effector Cartesian coordinates, g = f−1 $\mathbb{R} \rightarrow \mathbb{R}^n$ such that:

$$q = g(x) = f^{-1}(x), \quad x \in \mathbb{R}^m \ , q \in \mathbb{R}^n$$

To define the direct kinematic model, homogeneous transformations are used.

A robotic manipulator is a mechanism composed by a chain of links (i.e. rigid bodies) connected by joints. A reference frame is associated to each link and homogeneous matrices are used to describe their relative position and orientation. The reference frames are assigned according to the Denavit-Hartenberg (D-H) convention which allows to describe position and orientation of a 3D rigid body with only four parameters.

Once the D-H parameters of a manipulator with n+1 links are defined, the homogeneous transformation matrices between frame i-1 and i (i−1Hi, i = 1...n), are computed and then, the direct kinematic model can be found setting

$f = {}^0T_n$, with ${}^0T_n = {}^0H_1 {}^1H_2 ... {}^{n-1}H_n$.

The inverse kinematic problem does not have a unique solution; indeed in general the equation system modelling the problem can have no solution, a finite set of solutions or infinite solutions.

In order to obtain a closed form solution to the inverse kinematic problem, two approaches are possible: an algebraic approach or a geometrical approach. The first considers the elaboration of the kinematic equations until a suitable set of simple equations is obtained for the solution while the geometric approach is based, when possible, on geometrical considerations.

It analyzes the kinematic structure of the manipulator as a physical characteristic or workspace and provides constraints and boundary conditions that may help in the solution.

### 2.3.2 Dynamic Model

The relationship between mass and inertia properties, motion, and the associated forces and torques is studied as part of robot dynamics.

The dynamic model establishes the relationships between the motion and the forces involved, taking into account the masses and moments of inertia. Similarly to kinematics, also for the dynamics it is possible to define two "models": the direct model and the inverse model.

The direct dynamic model once the forces/torques applied to the joints, as well as the joint positions and velocities are known, compute the joint accelerations:

$$\ddot{\boldsymbol{q}} = \boldsymbol{f}(\boldsymbol{q}, \dot{\boldsymbol{q}}, \boldsymbol{\tau})$$

$$\dot{\boldsymbol{q}} = \int \ddot{\boldsymbol{q}}\, \boldsymbol{dt}$$

$$\boldsymbol{q} = \int \dot{\boldsymbol{q}} \boldsymbol{dt}$$

The inverse dynamic model, once the joint accelerations, velocities and positions are known, compute the corresponding forces/torques

$$\tau = f^{-1}(\ddot{q}(t), \dot{q}(t), q(t)) = g(\ddot{q}(t), \dot{q}(t), q(t))$$

Normally, a manipulator is composed by an open kinematic chain, and its dynamic model is effected by several "drawbacks" like low rigidity (elasticity in the structure and in the joints) and potentially unknown parameters (dimensions, inertia, mass. . .) or dynamic coupling among links. Other nonlinear effects are usually introduced by the actuation system is friction or dead zones and excreta (i.e. the range of input signals that do not generate an output in the system). For these reasons, in the derivation of the dynamic model, it is necessary to make an approximation of the system to an ideal case of a series of connected-rigid bodies.

There are several reasons for studying the dynamics of a manipulator:

- Simulation: test desired motions without resorting to real experimentation
- Analysis and synthesis of suitable control algorithms
- Analysis of the structural properties of the manipulator since the design phase.

Two approaches for the definition of the dynamic model: the Euler-Lagrange method and the Newton-Euler approach.

The Euler-Lagrange formulation is an energy-based approach which uses the kinetic K(q,q̇) and potential P(q) energies of the system as a starting point on the formulation of its equations of motion. It is a closed-form model since the solution is computed in an analytical way:

$$\tau = \frac{d}{dt}\frac{\partial L(q,\dot{q})}{\partial q_i} - \frac{\partial L(q,\dot{q})}{\partial q_i} \quad , i = 1 \ldots . n$$

Where:

$$L(q,\dot{q}) = K(q,\dot{q}) - P(q)$$

The Newton-Euler approach is based on analysis of forces and moments due to constraints acting between links. It first computes the angular velocity (ω), angular acceleration (ω̇), linear velocity (v) and linear acceleration (v̇) of each link in terms of the preceding link and then computes the joint forces F , one link at time, starting from the end-effector link and ending at the base link. It is a computationally efficient recursive technique but it is not expressed in a closed-form:

$$F = m\dot{v}$$

$$M = I\dot{\omega} + \omega \times I\omega$$

Where:

F is the force causing the acceleration,

M is the moment causing the rotation,

m is the mass, and

I is the moment of inertia.

The two techniques are equivalent and provide the same results, that is, they deduce the elements of the inertia matrix M (q), of the Coriolis and centrifugal forces matrix C (q,q̇) and of the elements of the gravity vector N (q).

$$\tau = M(q)\ddot{q} + C(q,\dot{q}) + N(q) + \tau_f(\dot{q})$$

Where:

$\tau_f$ is the friction component.

### 2.3.3 Cerebellum Inspired Module

An Artificial Neural Network (ANN) is an information processing paradigm that is inspired by the way biological nervous systems, such as the brain, process information. The key element of this paradigm is the novel structure of the information processing system. It is composed of a large number of highly interconnected processing elements (neurons) working in unison to solve specific problems. ANNs, like people, learn by example. An ANN is configured for a specific application, such as pattern recognition or data classification, through a learning process. Learning in biological systems involves adjustments to the synaptic connections that exist between the neurons. This is true of ANNs as well.

Neural networks, with their remarkable ability to derive meaning from complicated or imprecise data, can be used to extract patterns and detect trends that are too complex to be noticed by either humans or other computer techniques. A trained neural network can be thought of as an "expert" in the category of information it has been given to analyses. This expert can then be used to provide projections given new situations of interest and answer "what if" questions. Other advantages include:

- Learning: An ability to learn how to do tasks based on the data given for training or initial experience.
- Self-Organization: An ANN can create its own organization or representation of the information it receives during learning time.
- Real Time Operation: ANN computations may be carried out in parallel, and special hardware devices are being designed and manufactured which take advantage of this capability.
- Fault Tolerance via Redundant Information Coding: Partial destruction of a network leads to the corresponding degradation of performance. However, some network capabilities may be retained even with major network damage.

Multilayer FeedForward networks and recurrent networks are two forms of neural network architectures used in robotics. A multilayer perceptron (MLP) is a FeedForward artificial neural network model that maps sets of input data onto a set of appropriate outputs. The number of layers is the number of layers of perceptrons .They can learn many behaviors / sequence processing tasks / algorithms / programs that are not learnable by traditional machine learning methods. A MLP consists of multiple layers of nodes in a directed graph, with each layer fully connected to the next one. Except for the input nodes, each node is a neuron (or processing element) with a nonlinear activation function. MLP utilizes a supervised learning technique called back propagation for training the network.

Many different types of neural networks have been implemented in robotic system control, like trajectory control, feedback linearization and control error compensation.

In the robot control, neural network controllers are traditionally used to generate a compensating joint torque to account for the effects of the uncertainties in the non-linear robot dynamic model. Another application of this type of controller is to improve performances using the neural network as a non-linear filter; it acts as the inverse model of the plant and it can be trained on-line with joint errors.

Spiking neural networks (SNNs) is third generation of neural network models, increasing the level of realism in a neural simulation. In addition to neuronal and synaptic state, SNNs also incorporate the concept of time into their operating model. The idea is that neurons in the SNN do not fire at each propagation cycle (as it happens with typical multi-layer perceptron networks), but rather fire only when a membrane potential an intrinsic quality of the neuron related to its membrane electrical charge reaches a specific value. When a neuron fires, it generates a signal which travels to other neurons which, in turn, increase or decrease their potentials in accordance with this signal.

In the context of spiking neural networks, the current activation level (modeled as some differential equations) is normally considered to be the neuron's state, with incoming spikes pushing this value higher, and then either firing or decaying over time. Various coding methods exist

for interpreting the outgoing spike train as a real-value number, either relying on the frequency of spikes, or the timing between spikes, to encode information.

This kind of neural network can in principle be used for information processing applications the same way as traditional artificial neural networks. However due to their more realistic properties, they can also be used to study the operation of biological neural circuits. Starting with a hypothesis about the topology of a biological neuronal circuit and its function, the electrophysiological recordings of this circuit can be compared to the output of the corresponding spiking artificial neural network simulated on computer, determining the plausibility of the starting hypothesis.

# 3. The Project and the Specific Goals of This Work

**What is the REALNET**?

Realnet (http://www.realnet-fp7.eu/) is a European project about Realistic real-time Networks and computation dynamics in the cerebellum. In this project, they develop specific chips and imaging techniques to perform neurophysiological recordings from multiple neurons in the cerebellar network and monitor its Spatio-Temporal dynamics. Based on the data, they develop the first realistic real-time model of the cerebellum and connect it to robotic systems to evaluate circuit functioning under closed-loop conditions. The data deriving from recordings, large-scale simulations and robots will be used to explain the implicit dynamics of the circuit through the adaptable Spatio-Temporal filter theory. REALNET, through its network architecture based on realistic neurons, will provide a radically new view on dynamic computations in central brain circuits laying the basis for new technological applications in sensory-motor control and cognitive systems.

Cerebellum model Embed different plasticity rules and adaptation scales, in direct, which can be shown learning in different sensorimotor tasks carried out by a neurorobot.

Different protocols for stressing the role of the cerebellum have been designed and implemented; some of them like the force field perturbations, and the obstacle avoidance, before have been tested; in my work I focus these two protocols:

- Vestibulo-ocular reflex (VOR)
- EBCC (Eye blinking classic conditioning)

The goal of this project is the development of a brain inspired controller through the design and the implementation of a robotic platform in order to test the learning properties of the controller in cerebellar-driven tasks and to simulate the sensorimotor mechanisms.

## 3.1 Computational Model of the Cerebellum

Synaptic plasticity is the ability of synapses to strengthen or weaken during the time, in response to increases or decreases in their activity. Plastic change also results from the alteration of the number of receptors located on a synapse. There are several underlying mechanisms that cooperate to achieve synaptic plasticity, including changes in the quantity of neurotransmitters released into a synapse and changes in how effectively cells respond to those neurotransmitters. Synaptic plasticity in both

excitatory and inhibitory synapses has been found to be dependent upon postsynaptic calcium release. Since memories are postulated to be represented by vastly interconnected networks of synapses in the brain, synaptic plasticity is one of the important neurochemical foundations of learning and memory.

The cerebellar system implemented and embedded into the whole control system takes into account the major functional hypotheses that each cerebellar layer endows. It models Mossy Fibers (MF), Granular layer (GR), Inferior Olive (IO), Purkinje cell layer (PC) and Deep Cerebellar Nuclei (DCN). These cerebellar layers are inter connected, as shown in Fig 6 where Parallel Fibers (PF) are the axons of GR cells and the Climbing Fibers (CF) come from the Inferior Olive (IO).

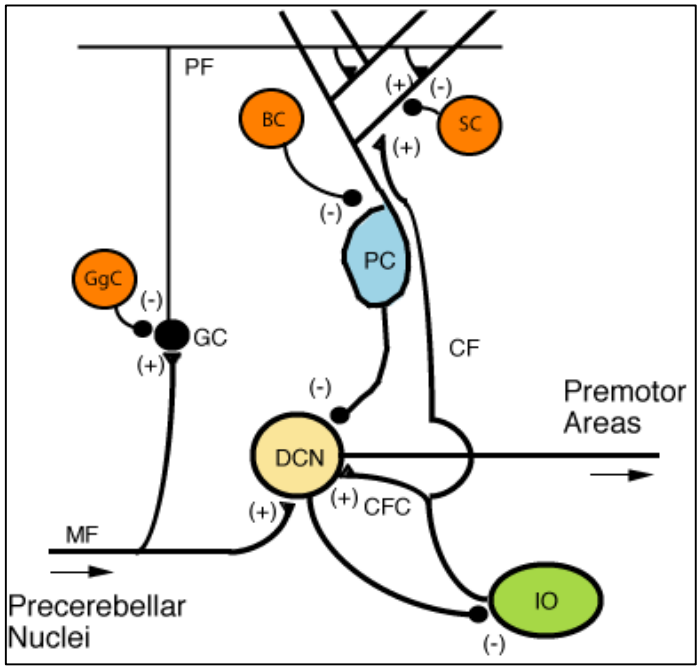


*Figure 6: The plasticity sites*

The Granular layer is modeled as a state generator; it identifies each time state for each task repetition i.e. there is one parallel fiber for each time sample of the trial. The large number of granular cells (and then of their axons, i.e. PF) guarantees a reliable pattern separation, which means that similar input patterns would be sparsely re-encoded into largely not-overlapping populations of granular cells activity. The number of parallel fibers defined in the model changes with the task to be tested. The granular layer was hypothesized to perform expansion recoding of input signals and the PF-PC synapse to learn and store relevant patterns under the control of the teaching signal provided by CFs. On the basis of electrophysiological determinations, it has been suggested that the inferior olive, by comparing proprioceptive and predicted signals, is indeed able to provide quantitative error estimation [25].

The model considers a constant firing rate from mossy fiber (MF (t) =1) multiplied by a "gain" which represents MF→DCN synapses. Indeed, it is assumed that this constant input to the granular layer circuit does not affect its capability to generate time-evolving states. The PC layer has been suggested to correlate the PF input activity with the CF error-based teaching signal [26]. It associates

the actual state with an output firing rate learned along the trial and it drives the PF→PC long-term plasticity. The activity of the PC layer is defined as follows:

$$PC_i(t) = f_i\big(PF(t)\big)\ , i = 1,2, \dots number\ of\ muscles$$

Where $PC_i(t)$represents the firing rate of the PCs associated with the (i-th) muscle and $f_i$ associates each granular layer state (i.e., one active PF) with a particular output firing rate at the (i-th) PC.

The DCN cells integrate the excitatory activity coming from MFs and the inhibitory activity coming from PCs. By linearly approximating the influence of excitatory and inhibitory synapses on DCN firing rate, the output of the DCN cell population was described as follows:

$$DCN_i(t) = W_{MF-DCN_i} - PC_i(t).W_{PC_i-DCN_i}\ ,\quad i = 1,2, \dots number\ of\ muscles$$

Where $DCN_i(t)$ represents the average firing rate of the DCN cell associated with the (i-th) muscle, $W_{MF-DCN_i}$ is the synaptic strength of the MF-DCN connection at the (i-th) muscle, and $W_{PC_i-DCN_i}$ is the synaptic strength of the PC-DCN connections at the (i-th) muscle. Thus, the DCN layer was implemented as an adder/subtracted and the afferent activity coming from the MFs and PCs was scaled by synaptic strengths (MF-DCN and PC-DCN synapses, respectively).

These synaptic weights were progressively adapted during the learning process. It is important to note the absence of an MF activity term. We assume a constant input rate from MFs during the learning process. Thus, the excitatory component of the DCN firing rate is dependent only on the MF-DCN synaptic weight.

**PF-PC** synaptic plasticity is the most widely investigated cerebellar plasticity mechanism and different studies have supported the existence of multiple forms of LTD and LTP. The main form of LTD [27] is heterosynoptically driven by CF activity, and is therefore related to the complex spikes generated by CFs, while the main form of LTP [28] is related to the simple spikes generated by PFs. The present model implements PF-PC synaptic plasticity as follows:

$$\Delta W_{PF\,j} - PC_i(t) = \begin{cases} \dfrac{LTP_{Max}}{(\varepsilon_i(t)+1)^{\alpha}} - LTD_{Max}.\varepsilon_i(t) & if PF_j\ is\ active\ at\ t\ , i = 1,2, \dots. \\ 0 & otherwise \end{cases}$$

Where $\Delta W_{PF_j} - PC_i(t)$ is the weight change between the (j-th) PF and the target PC associated with the (i-th) muscle, εi is the current activity coming from the associated CF (which represents the normalized error along the executed arm plant movement), LTPMax and LTDMax are the maximum LTP/LTD values, and α is the LTP decaying factor. LTD was generated proportionally to the incoming error signal through CFs, LTP was constantly generated when spikes reached the target PC .The α was set at 1000 thus allowing a fast decrease of LTP and preventing early plasticity saturation (Figure 7).

**MF-DCN** synaptic plasticity, which has been reported to depend on the intensity of DCN cell excitation, was implemented as [29]:

$$\Delta W_{MF-DCN_i}(t) = \frac{LTP_{Max}}{(PC_i(t)+1)^{\alpha}} - LTD_{Max}.PC_i(t)$$

Where $\Delta W_{MF-DCN_i}(t)$ represents the weight change between the active MF and the target DCN associated with the (i-th) muscle, $PC_i(t)$ is the current activity coming from the associated PCs, LTPMax, and LTDMax are the maximum LTP/LTD values, and α is the LTP decaying factor.

In order to maintain the stability of the learning process, the LTPMax and LTDMax values had to be lower than those defined at the PF-PC synapse. PF-PC plasticity was driven by CF activity, MF-DCN plasticity was driven by PC activity.

This mechanism can optimize the activity range in the whole inhibitory pathway comprising MF-PF-PC-DCN connections: high PC activity causes MF-DCN LTD, while low PC activity causes MF-DCN LTP.

This mechanism implements an effective cerebellar gain controller, which adapts its output activity to minimize the amount of inhibition generated in the MF-PF-PC-DCN inhibitory loop.

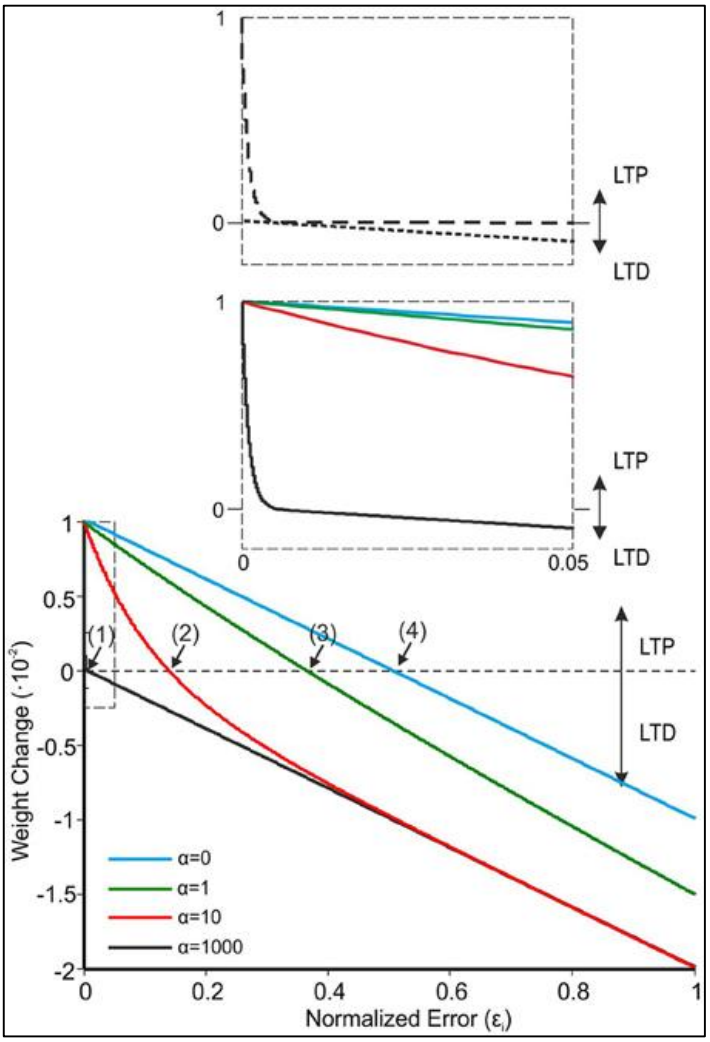


*Figure 7: The learning rule for PF-PC plasticity [30].*

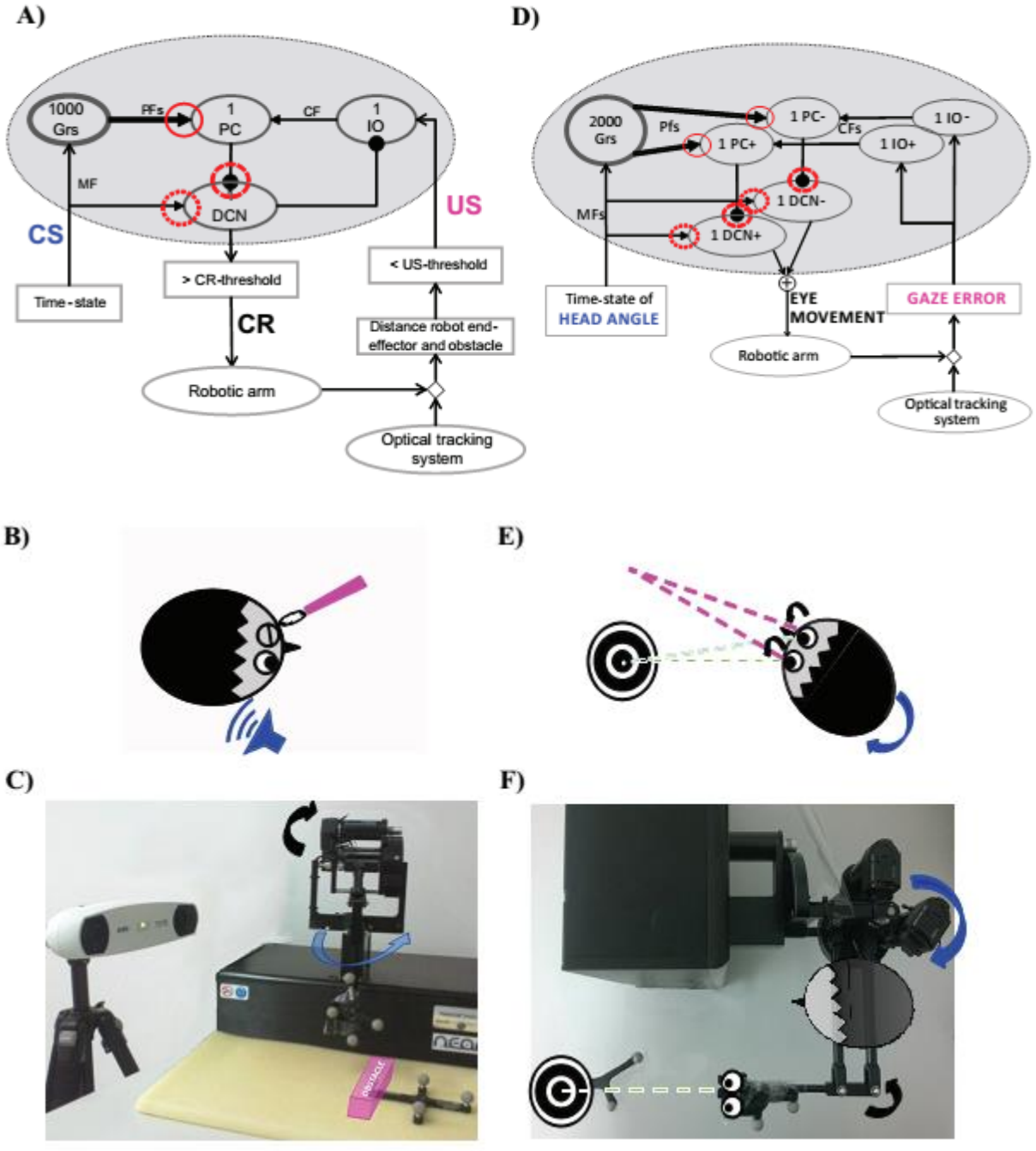


*Figure 8: Embodied cerebellar model and set-up (A): cerebellar model embedded into the neurorobot, with EBCC-specific input and output signals. The red circles represent the plasticity sites: straight line the PF-PC synapses; dot line and dashed line the MF-DCN and PC-DCN synapses, respectively, activated only within the 3-plasticity model. Arrows represent excitatory connections, whereas dot-arrows inhibitory connections. The EBCC-like Pavlovian task is reproduced into the robotic platform by defining the onset of the US stimulus based on the distance between the moving robot end-effector and the fixed obstacle placed along the trajectory (US-threshold), detected by the optical tracker. CS, fed into the CF pathway, represents the system time-state, decoded by the GR layer. CS and US coterminate "delay EBCC". The DCN triggers the conditioned response (CR). (B): human-like EBCC task. (C): robotic set-up reproducing the Pavlovian EBCC-like task. (D): cerebellar model with VOR-specific input and output signals. The red circles represent the plasticity sites:*

*straight line the PF-PC synapses; dot line and dashed line the MF-DCN and PC-DCN synapses, respectively, activated only within the 3-plasticity model. Arrows represent excitatory connections, whereas dot-arrows inhibitory connections. The VOR is reproduced into the robotic platform by using the second joint of the robotic arm as the head (imposed rotation) and the third joint (determining the orientation of the second link, on which the green laser is placed) as the eye. The dis alignment between the gaze direction (i.e. second link orientation) and the environmental target to be looked at is computed through geometric equations from the optical tracker recording. Head vestibular stimulus represents the system time-state, decoded by the GR layer. The gaze error is fed into the CF pathway, the DCN modulate the compensatory eye movement. (E): human-like VOR task. (F): robotic set-up reproducing the VOR task.*

**PC-DCN** synaptic plasticity was reported to depend on the intensity of DCN cell and PC excitation and was implemented as [31]:

$$\Delta W_{PC_i-DCN_i}(t) = \frac{LTP_{Max}.PC_i(t)^{\alpha}}{(DCN_i(t)+1)^{\alpha}} - LTD_{Max}.(1-PC_i(t))$$

Where $\Delta W_{PC_i-DCN_i}(t)$ is the synaptic weight adjustment at the PC-DCN connection reaching the DCN cell associated with the (i-th) muscle. PCi(t) is the current activity coming from the associated PC (in the range [0,1]), DCNi(t) is the current DCN output of the target DCN cell, and α represents the decaying factor of the LTP (again, it was set at 1000 as in MF-DCN and PF-PC learning rules).

This learning rule led the PC-DCN synapses into a synaptic weight range appropriate to match the synaptic weight range at PFs. the equation above caused LTP only when both the PCs and their target DCN cell were simultaneously active.

For both tasks we have applied two controllers, embedding two different cerebellum model:

1) Single Plasticity Site : only PF-PC
2) Three Plasticity Sites: PF-PC, MF-DCN, PC-DCN.

# 4. Hardware and Software

Modeling the cerebellar structure and embedding it into the control of a real robot immersed into real-world conditions is a key approach to associate the detailed model of neuronal connectivity and synaptic plasticity with behavioral functionalities. Experiments with real robots allow the exploration of the robustness and generalization of the controlling model [32].

## 4.1 Robotic Platform

As you can see in the Figure 9, the main robot is a Phantom Premium 1.0 (SensAble™), a lower friction haptic device with 3 rotational Degrees of Freedom (DoFs). It is equipped with digital encoders at each joint and it can be controlled with force and torque commands. It is integrated with a motion capture device, a VICRA-Polaris (NDI™),in figure 9 which is an optical measurement system acquiring marker-tools at 20 Hz.

*Figure 9: Phantom Premium 1.0 SensAble Technologies®.*

Visual information from both the internal and the external environment has been handled thanks to the IGSTK libraries (http://www.igstk.org/). When the visual integration is necessary, wireless passive tools are placed in correspondence of the robotic end-effector and of the objects of interest in the environment. In order to allow the match of information carried by signals from the tracking device (Visual system Vr) and the robot (Proprioceptive system Pr), a-priori calibration has been defined which itself identifies the constant Roto-translation between the reference systems of the two devices.

*Figure 10: VICRA Polaris® NDI*

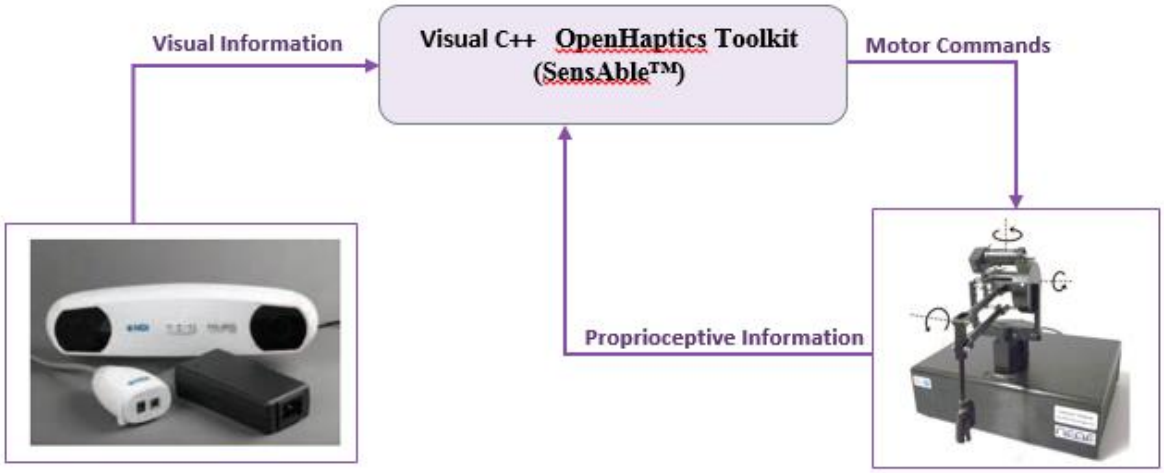


*Figure 11: The implemented robotic platform with hardware and software components*

The controller of robotic platform has been developed in Visual C++.

As we explain that before the hardware is the Phantom Premium 1.0 from the SensAble Technologies® which displays higher fidelity, stronger forces, and lower friction respect older version of that. Phantom Premium 1.0 have 3 DoF haptic devices with three active rotational joints and two links. It is provided with digital encoders which measure the Cartesian position of the end-effector or the angle of each joint, and they can be controlled through force or torque commands. Each of the three arm joints is driven by a Maxon 118743 DC brushed motor with a shaft-mounted HEDM-5500-B02 optical encoder. Drum and capstan cable drives are used to connect the motors to the respective joints. Torques from the motors are transmitted through pre-tensioned reduction cables to a stiff, lightweight aluminum linkage. At the end of this linkage there is a passive, three degrees of freedom gimbal attached to a thimble. Because the three passive rotational axes of the gimbal coincide at a point, there can be no torque about that point, only a pure force.it has been designed so that the transformation matrix between motor rotations and endpoint translations is nearly diagonal.

An interesting design feature of the Phantom Premium 1.0 is that two of the three motors move in such a manner as to counterbalance the linkage structure. Because the Phantom Premium 1.0 is statistically balanced, there is no need to compromise the dynamic range of the device by actively balancing the structure with biased motor torques. Conveniently, the first rotational axis of the Phantom Premium 1.0 is located directly above the wrist of the user. This permits aligning the inherently spherical workspace of the mechanism with similarly spherical wrist. The complexity of the cable reduction mechanism is minimized by using a single cable to "mesh" two motor capstans with another pulley. This minimizes mechanism width and tensioning difficulty. In conclusion, the Phantom Premium 1.0 can be considered a joint low friction haptic device with low inertia and high stiffness.

Another device is the VICRA Polaris® an optical measurement system which gets 3D positions of active and passive markers applied to specific tools. Passive markers are highly reflective spheres,

which reflect the light emitted through a ring of IRED positioned around the Polaris® sensors. The light is captured from the cameras and through the col linearity equations the coordinates in the 2D sensor planes are related to the object coordinates (in three dimensions).It connects to the computer via the USB 2.0 port and its maximum update rate is 20Hz. The technical specifications of these instruments are compatible with the slower refresh of the visual information compared to the vestibular and proprioceptive information (state of the system provided by joint encoders).

The controller was developed in Visual C++, exploiting the OpenHaptics™ Toolkit and the Image-Guided Surgery Toolkit (IGSTK).

**Phansim© Toolkit**: The controller has been developed exploiting the OpenHaptics Toolkit (SensAble™) and the Image-Guided Surgery Toolkit (IGSTK). In the OpenHaptics Toolkit, the Haptic Device Application Programming Interface (HDAPI) provides low-level access to the haptic device allowing torque signals to be sent to the robotic DoFs and signals from the encoders to be received. In order to guarantee stability, the control loop must be executed in a separate, high-priority thread at 1 kHz rate. The hdSet and the hdGet functions have been included in the main code of the controller and integrated with different algorithms developed to run the experiments. Depending on the protocols, the number of employed DoFs has been changed.

**OpenHaptics™ Toolkit**: The OpenHaptics™ enables users to add haptics and true 3D navigation to a broad range of applications. It is a haptic library developed by SensAble Technologies® and it is intended to ease adoption of haptics technology. This toolkit has a layered architecture composed by the Haptic Device Application Programming Interface (HDAPI) which provides low-level functions for device access offering control over configuring the runtime behavior of the drivers and the Haptic Library Application Programming Interface (HLAPI) that handles the collision detection and response for haptic rendering of shapes and effects. In order to implement the torque control strategy, the computed motor commands are sent as joint torques by setting the HD_CURRENT_JOINT_TORQUE parameter, which allows full torque control of the Phantom device in the joint space domain. The servo loop refers to the tight control loop used to calculate forces/torques to send to the haptic device. For stability, this loop must be executed at a consistent 1 kHz rate which is possible thanks to the Scheduler. This mechanism is embedded in the HDAPI and it facilitates thread-safe synchronization between threads (i.e. HDCALLBACKS). In order to maintain such a high update rate, the servo loop is thus executed in these high-priority threads.

**Image-Guided Surgery Toolkit** Image-Guided Surgery Toolkit (IGSTK) is an Open Source software toolkit (http://www.igstk.org/) designed to facilitate the development of image-guided surgery applications. In the controller development, the low-level libraries related with the integration of optical trackers have been embedded. IGSTK is developed on top of other toolkits (ITK, VTK, FLTK). All of them are C++ software systems. The main steps include activating the serial communication with the tracker, “attaching” the defined tools to be tracked and reading the position and orientation of each tool (transform) at a defined frequency (20Hz). The tracking procedure is triggered by “observer” elements able to listen to the transform events. Each desired tool to be tracked is identified by a .rom file, which defines the unique geometry of the reflective markers composing the tool itself.

# 5. Protocol Design and Tests

Two different protocols stressing the role of the cerebellum have been designed and implemented the VOR and the EBCC. The VOR create eye movements which aim at stabilizing images on the retina during head movement. It's tuning the main attribute to the cerebellum loop. The learning is based on the two stimuli temporal association, head turn and motion of retinal image, i.e. the system learns that one stimulus will be followed by another stimulus and a in the resulting predictive compensatory response is slowly produced and accurately tuned [20]. The Eye-blink conditioning is an example of related learning in which a puff of air act as unconditioned stimulus (US) that evokes a reflex eyelid response and it is always predicted by a tone which act as conditioned stimulus (CS). If CS-US pairs are issued, with repetitions, an eye-blinking response is slowly expanded until the tone evokes a learned eyelid response even without US. The main feature of EBCC is that the temporal conjunction of two stimuli causes learning, thus it is a temporal associative learning. The cerebellum learns that one stimulus (tone) will be followed by another stimulus (air puff) and uses this information producing an anticipatory response (eye-blink). Thus the cerebellum learns the correct timing of the response. Moreover, the role of additional two plasticity site in controlling cerebellar learning in eye-blink conditioning has been demonstrated [33].

**Learning by cerebellum network with single plasticity site:**

First we consider the single site synaptic Plasticity PF-PC, In particular as the learning rule,PF-PC plasticity operated as a time correlation between the actual input state and the system error. This synaptic plasticity is occurred in the cerebellar cortex and generated LTP and LTD.

By some experiences the values for single plasticity has been obtained:

LTPMax=0.01 and LTDMax=0.04.

**Learning by cerebellum network with three plasticity site:**

The LTPmax and LTDmax of each plasticity site could be tuned. Some constraints came from neurophysiology properties. In the 1st plasticity site (PF-PC), LTPmax has to be lower than LTDmax, otherwise LTP, constantly generated when a state-related activity come from GRs, could counterbalance and nullify LTD effects. Moreover, to maintain the stability of the learning process, LTPmax and LTDmax values of the other two plasticity rules have to be lower than those defined at the PF-PC synapses.

The following values have been set for three plasticity sites:

- (PF-PC) → $LTP_{Max}=0.01$ and $LTD_{Max}=0.04$
- (MF-DCN) → $LTP_{Max}=3\times10^{-6}$ and $LTD_{Max}=5\times10^{-8}$
- (PC-DCN) → $LTP_{Max}=2\times10^{-6}$ and $LTD_{Max}=2\times10^{-6}$

## 5.1 VOR (Vestibulo-Ocular Reflex)

**Vestibulo ocular reflex** (VOR) is a reflex eye movement that stabilizes images on the retina during head movement by producing an eye movement in the direction opposite to head movement, thus preserving the image on the center of the visual field. For example, when the head moves to the right, the eyes move to the left, and vice versa. Since slight head movement is present all

the time, the VOR is very important for stabilizing vision: patients whose VOR is impaired find it difficult to read using print, because they cannot stabilize the eyes during small head tremors. The VOR does not depend on visual input and works even in total darkness or when the eyes are closed. However, in the presence of light, the fixation reflex is also added to the movement [34].

The VOR has both rotational and translational aspects. When the head rotates about any axis (horizontal, vertical, or torsional) distant visual images are stabilized by rotating the eyes about the same axis, but in the opposite direction. When the head translates, for example during walking, the visual fixation point is maintained by rotating gaze direction in the opposite direction, by an amount that depends on distance.

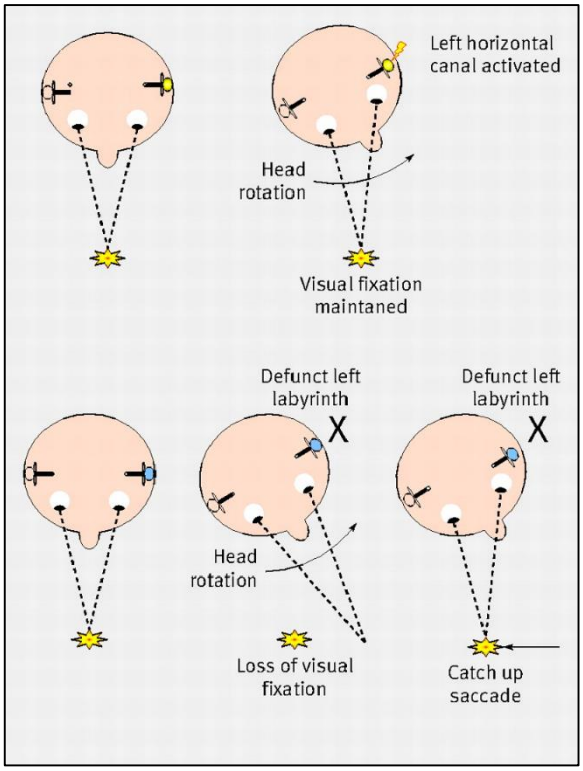


*Figure 12: Vestibulo ocular reflex*

The VOR consists of eye movements stabilizing images on the retina during head motion, and its tuning is ascribed mainly to the cerebellar flocculus [35].

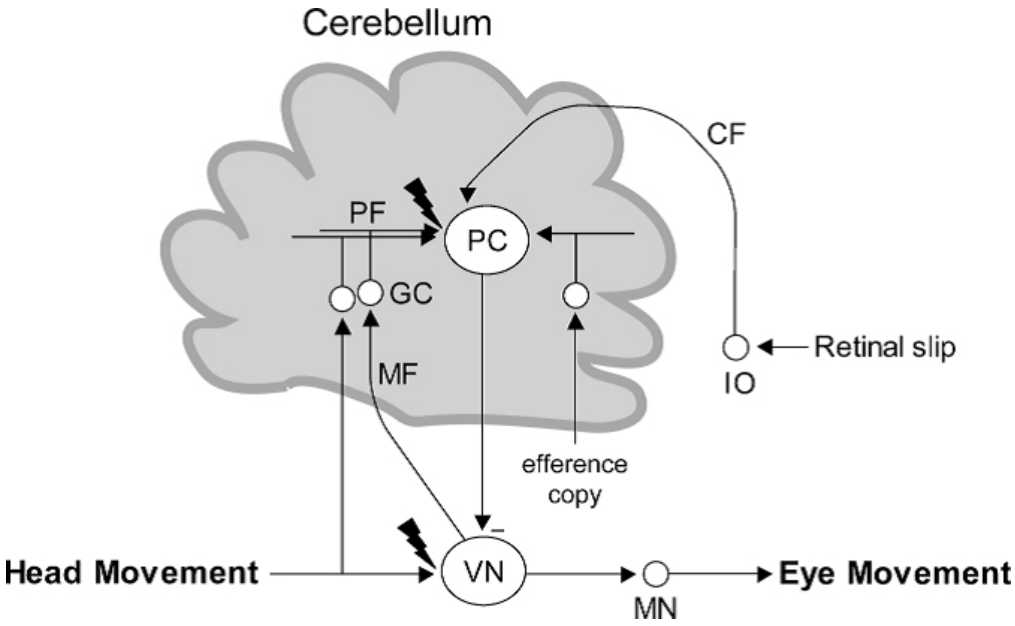


*Figure 13: Cerebellum Cell in VOR protocol*

### 5.1.1 Robotic implementation

For avoiding the gravitational effects in this protocol, the Phantom Premium 1.0 was rotated and used on a horizontal plane. The joint 1 is inactive and fit in the base of the robot. Because of the mechanical coupling of the device, the head rotation is imposed sending the appropriate torques to both joint 2 and joint 3, while the corrective torque resulting from learning is applied only to joint 3.we have two tools. One of them is attached to the ended of the premiums end-effector. Another one is the target .Both of them observed and record as an image by optical measurement system VICRA.

The VICRA system records the current position of the image as well as the End-effector of the Phantom Premium 1.0 on which another tool is attached.

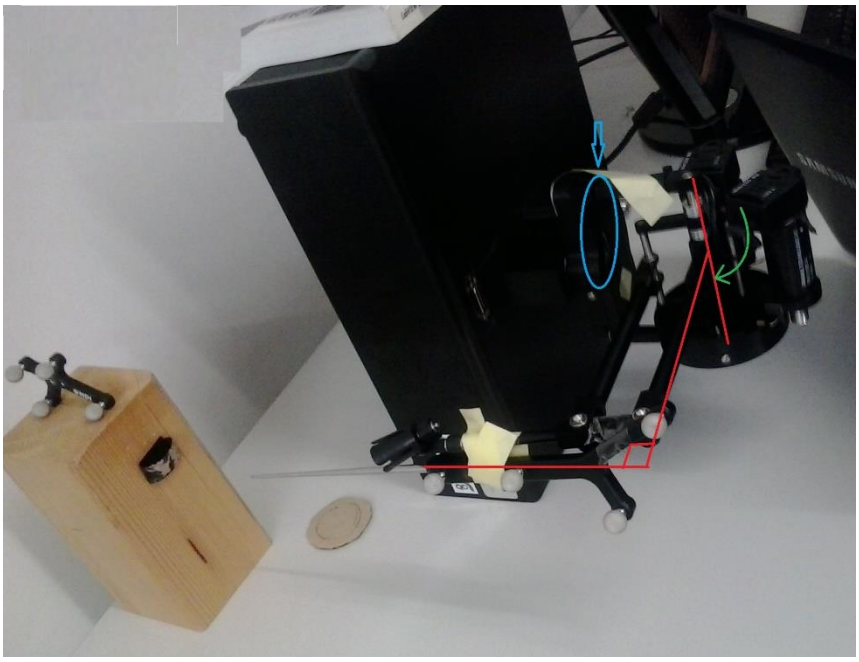

*Figure 14: premium robot in VOR protocol*

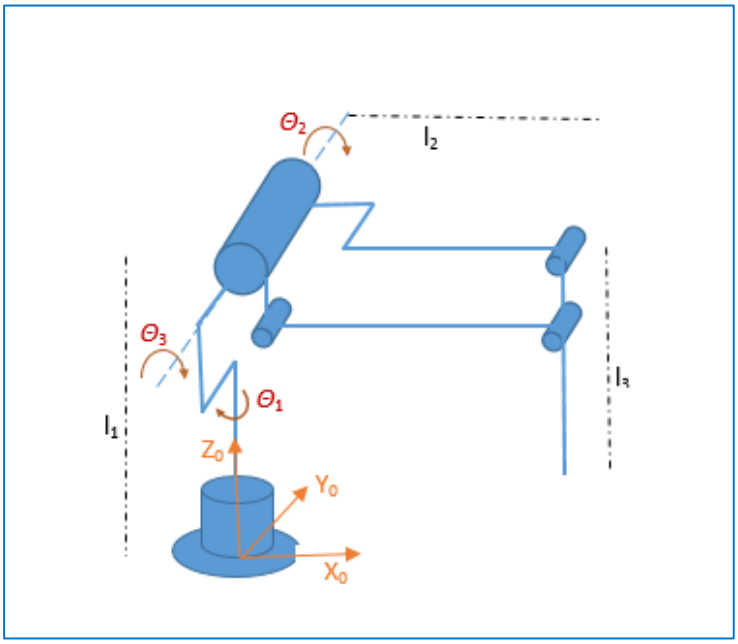


*Figure 15: links and joints of the Premium*

The cerebellum is triggered by the start of the head motion and receives the gaze error that computed by the gaze error algorithm. This algorithm computes the dis-alignment angle between the second link, which represents the gaze direction, and the tool that represents the target.

As shown in Figure 16 the angle (α) is found with the formulation below and considering to the segment which represents the second link , V, and the segment which links the center of the image-tool to the second joint , U.

$$\cos \propto = \frac{U.V}{\|U\|\|V\|}$$

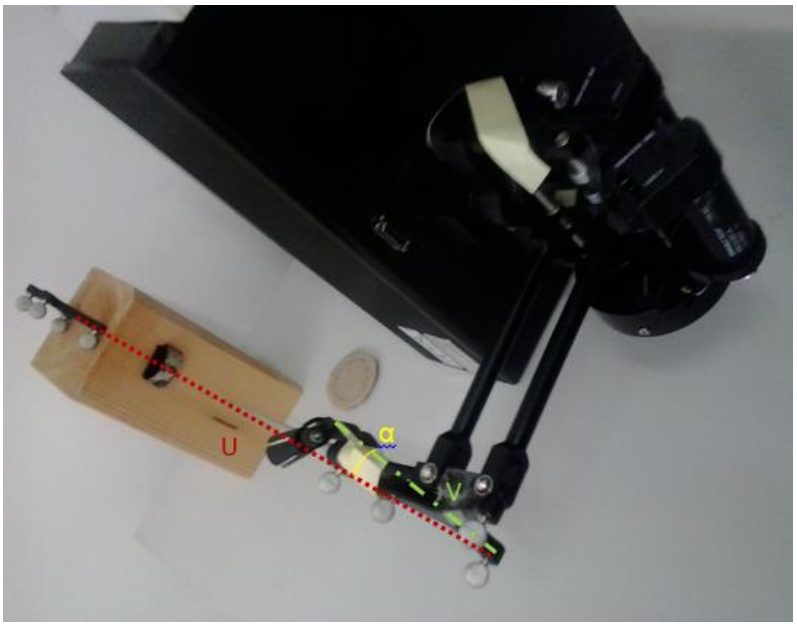


*Figure 16: The gaze error*

### 5.1.2 Learning by Cerebellum Network Result

Only joint 2 and 3 are activated in the vestibule-ocular reflex protocol. The cerebellum control only the third joint (number of the cerebellum joints).Different sequences of repetitions were tested, some parameters were kept constant in all the tests while others were changed depending on the task. In this experiment, the repetition duration step was consider 3000 milliseconds and the repetition duration time was 3 seconds.

The test was made up of two VOR sessions (session1 and session2) with fixed target. Each VOR session consisted of 40 trials of acquisition by imposing a pre-defined head rotation, directly followed by 20 extinction trials (head turn null).

In order to validate the robustness of the embedded cerebellar controller, different vestibular stimulus patterns, i.e. three Head Rotation (HR) profiles were set: HR1 = 25° in 2 seconds, HR2 = 30° in 2 seconds, HR3 = 35° in 2 seconds. For each HR, 15 tests were carried out.

In order to check the capacity to rapidly face changes of the stimulus, for each cerebellar controller, a second test was carried out. It reproduced initially the VOR session1with HR1 = 25° in 2

seconds, but during the steady plateau of the network outcomes (at the 35th trial of acquisition), gain-up stimulus was provided: the head rotation was increased 1.5 times, from 25° to 37.5°, and imposed for other 15 trials. Thus, the test was made up of 50 repetitions.

Gaze error and DCN activity were analyzed; since the protocol required a continuous shape modulation of the motor response, we focused on the Root Mean Square (RMS) of the net DCN activity (taking into account the net activity, DCN+ and DCN-) within each trial.

All tests were performed embedding the 1-plasticity cerebellum model (PF-PC) and the 3-plasticity model (PF-PC, MF-DCN, PC-DCN).

The vestibular stimulus onset, i.e. the onset of MF activity, started the generation of the granular layer state sequence and also provided the excitatory drive to DCN cells. The decoding of the gaze error reached continuously the Purkinje cells through the IOs. The Purkinje cells in turn inhibited the DCNs. At the beginning of the acquisition phase, Purkinje cell was spontaneously active, supplying tonic inhibition to the DCNs (Fig. 17.A).

After acquisition, PC+ activity was decreased; summing up all the presynaptic (constant or plastic) inputs to DCN+, DCN+ neurons began to fire so as to continuously counterbalance the head movement, minimizing the gaze error (Fig. 17.B). Then during extinction trials, PC activity was progressively re-increased; and DCN decreased the output motor commands actuating eye motion (Fig. 17.C).

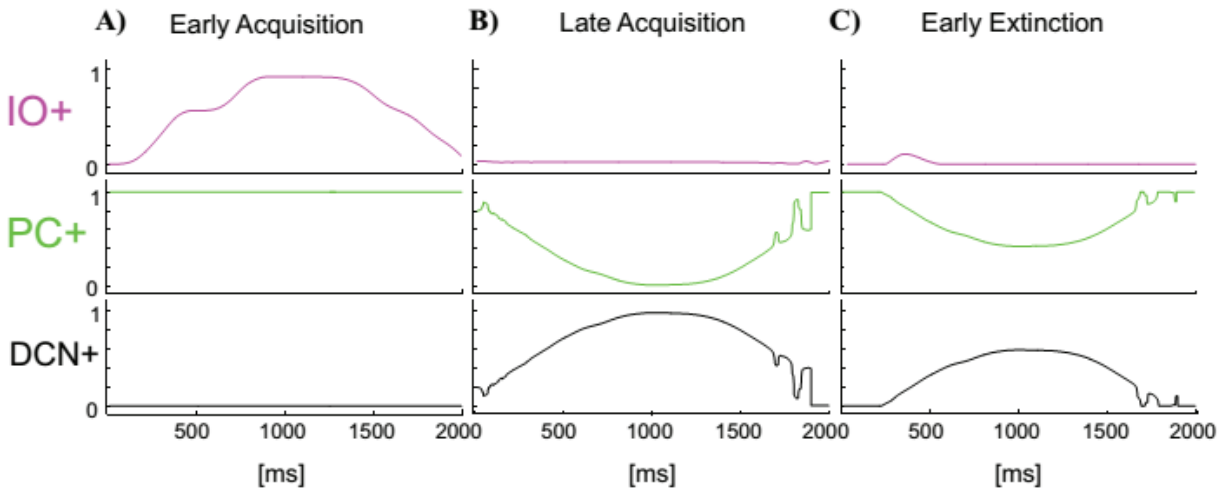


*Figure 17: Acquisition time in VOR*

The DCN output of the 3-plasticity model showed an evolution across sessions, while the DCN output of the 1-plasticity model repeated exactly the same adaptation process regardless any previous achieved acquisition (Fig. 18.A). Since the functioning of the cerebellum as predictive controller acting based on previous trials, during the extinction phases the after-effects occurred for few repetitions: even if the head rotation was canceled, the network output still produced eye

compensation; this overcompensation led to a gaze error with opposite sign (Fig. 18.B). Rapidly, the network learned to bring back the error to zero level.

The modulation of each plastic connection embedded into the cerebellar models represents the intrinsic mechanisms underlying these observed behaviors. For each trial, the PFs active without a correlated CF signal on the PC underwent an LTP, while PFs corresponding at the time-states when a signal arrived to the PC from CF developed LTD. All the 2000 PFs decoded system-state during head motion, thus corresponding to a not-null gaze error; they underwent to a proportional LTD, so spreading within the weight range (0-1) (Fig. 18.C, D, E, F). The PF-PC weights histograms (Fig. 18.C, D) clearly showed that in late acquisition, the same behavioral outcomes, i.e. steady eye motion perfectly compensating head motion, was achieved by different weight distributions between the two models.

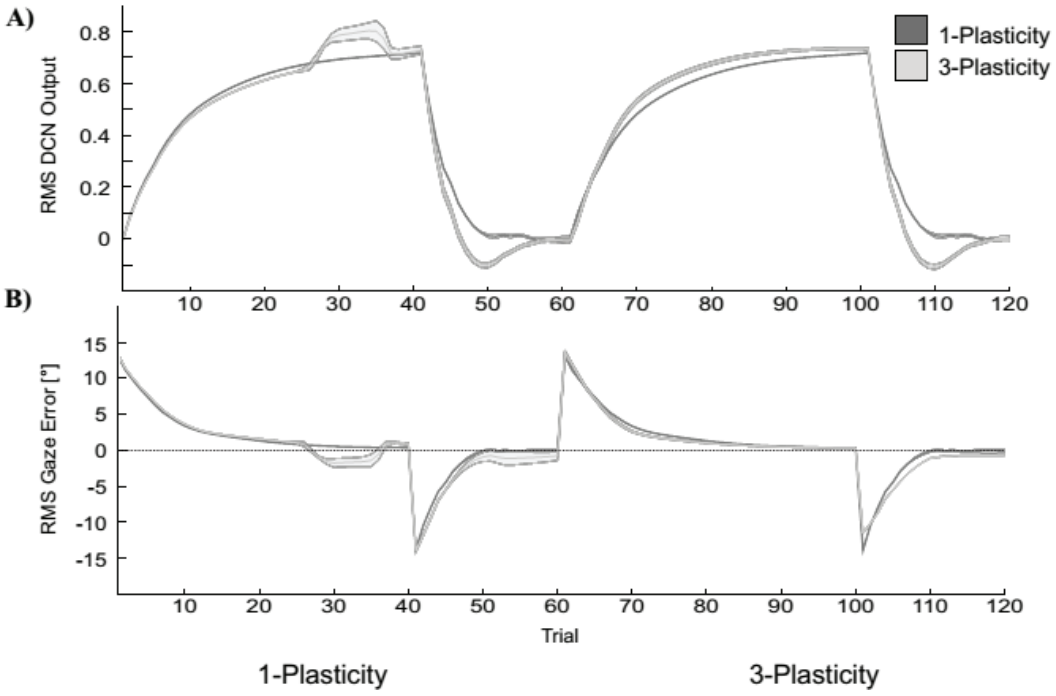


*Figure 18: RMS Gaze Error in one and three plasticity in VOR*

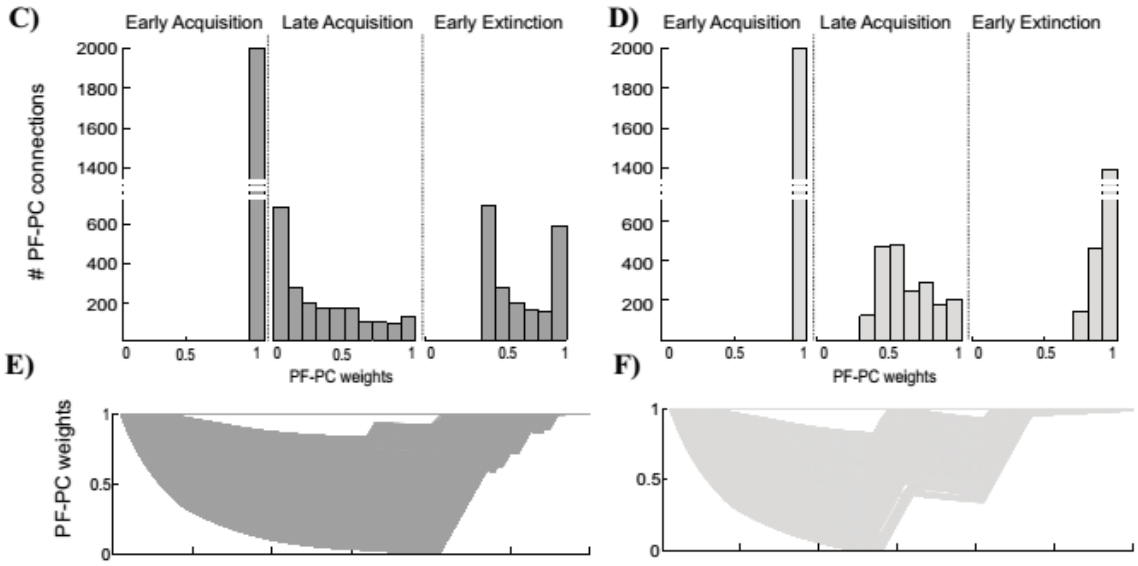


*Figure 18: PF-PC Weights and connections*

Most of these weights in the 1-plasticity controller was saturated at 0 level; whereas, in the 1-plasticity one, they were more distributed around half value of their range. The main phenomenon driving acquisition was the development of LTD at the synapses PF-PC; however, in the 3-plasticity model, in the meanwhile, with a slower rate, plasticity at the MF-DCN synapse and at the PC–DCN synapse occurred (Fig. 18.G, H, I, L). Thus a partial transfer of activity generating motor responses occurred from cortical to nuclear plasticity sites. These changes of weights at DCNs allowed to partially clear the cortical synapses. The network was then able to decrease the eye motion by fast PF-PC LTP, but without canceling the slower nuclear plastic changes had occurred. Thus, session2 controlled by the 3-plasticity model started with the cerebellar synapses in a different state than when controlled by the 1-plasticity model: the distributed plasticity dynamics, able to store information, was responsible for the higher learning rate in session2.

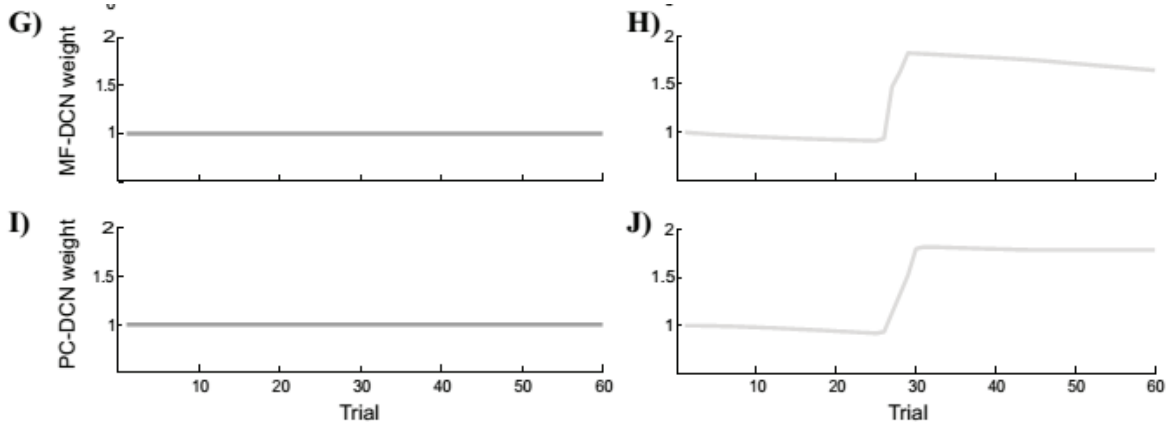


*Figure 18: PC-DCN Weights and connections*

The memory transfer effect pointedly arose in the gain-up VOR test (Fig. 19). Indeed, the passage from cortical to nuclear sites made the PF-PC synapses ready for further plasticity. In this way, they were able to react to other additive perturbations, suddenly presented to the system.

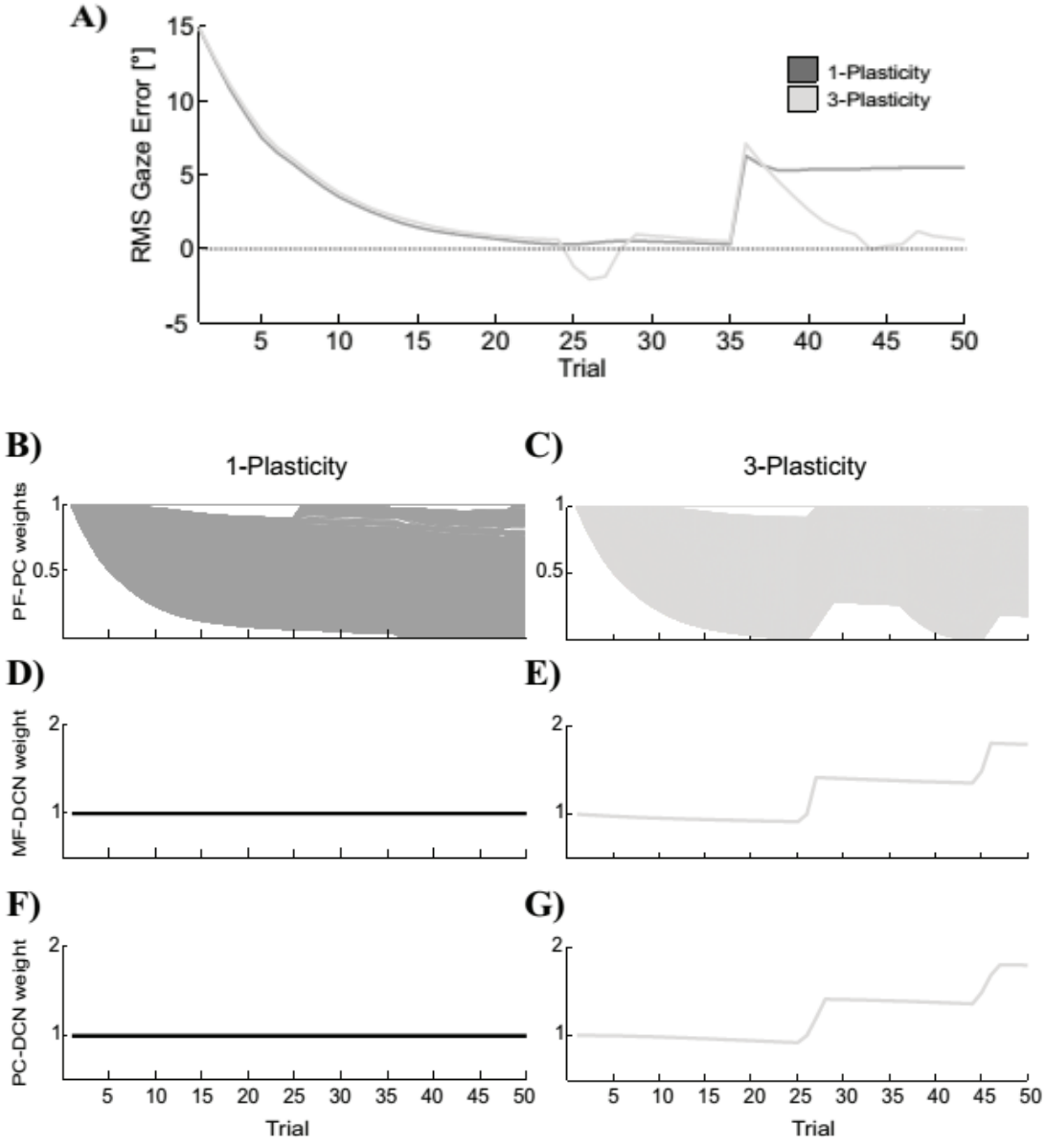


*Figure 19: RMS Gaze Error and weights of three synaptic plasticity*

In late acquisition, the performances of the two models were comparable, but the PF-PC synapses of the 1-plasticity controller were close to saturation. When the gain-up stimulus was provided, the 1-plasticity model exploited the residual cortical plasticity till complete saturation; it did not allow to an accurate eye compensatory movement. Whereas, the 3-plasticity model exploited the permanent nuclear changes and the much more residual plasticity at cortical level; it allowed to accurately recalibrate the eye motion.

## 5.2 EBCC (Eye Blink Classical Conditioning)

Eye blink classical conditioning (EBCC) is a form of classical conditioning that has been used extensively to study neural structures and mechanisms that underlie learning and memory. The procedure is relatively simple and usually consists of pairing an auditory or visual stimulus (the conditioned stimulus (CS)) with an eye blink-eliciting unconditioned stimulus (US) (e.g. a mild puff of air to the cornea or a mild shock). Naïve organisms initially produce a reflexive, unconditioned response (UR) (e.g. blink or extension of nictitating membrane) that follows US onset. After many CS-US pairings, an association is formed such that a learned blink, or conditioned response (CR), occurs and precedes US onset. The magnitude of learning is generally gauged by the percentage of all paired CS-US trials that result in a CR. Under optimal conditions, well-trained animals produce a high percentage of CRs (> 90%). The conditions necessary for, and the physiological mechanisms that govern, eye blink CR learning have been studied across many mammalian species, including mice, rats, guinea pigs, rabbits, ferrets, cats, and humans. Historically, rabbits have been the most popular research subjects [36].

In neuroscience, classical conditioning is typically studied by experiments on eye blink conditioning. In these experiments, rabbits (or rodents) associate an auditory tone (conditioned stimulus) with an air puff (unconditioned stimulus) to perform an eye blink (unconditioned response). Essentially, after multiple trials, the rabbit will eye blink in response to the tone alone.

Eye blink conditioning is now known to involve the cerebellum.

The anatomy of the cerebellum is well understood (figure 20). The major output regions of the cerebellum are the deep cerebellar nuclei: activation of these nuclei results in the activation of motor commands. These nuclei receive inputs from excitatory ascending fibers (mossy fibers, climbing fibers) that promote motor commands; they also receive inhibitory inputs from Purkinje cells that inhibit motor commands. Therefore, whether or not a motor command is executed depends on the level of activation of the deep cerebellar nuclei, which is in turn dependent on the activity of both mossy and climbing fibers as well as Purkinje neurons. Climbing fiber synapse is very strong on the Purkinje cell while the parallel fiber synapses on the Purkinje cell are very weak. We see this experimentally: parallel fiber response increases linearly with increased stimulation while the climbing fiber has more of an all or nothing response.

In classical conditioning, the conditioned stimulus (CS), a tone, will activate mossy fibers originating in the pontine nuclei that in turn send projections to granule cells in the cerebellar cortex. The synapses between mossy fibers and granule cells are excitatory: activation of the mossy fiber will result in activation of the granule cell. The axons of granule cells are termed parallel fibers and form excitatory synapses onto Purkinje cells, the major inhibitory neuron of the cerebellar cortex. The activation of the Purkinje neuron by granule cell results in inhibition of the deep cerebellar nuclei (the interpositus nuclei, according to the figure 20), which is the motor output region of the cerebellum. This inhibition will prevent any motor response by the animal.

The cerebellum learns the correct timing of the response. Therefore besides the other implemented paradigms, eye-blink conditioning allows only the timing aspect of learning to be focused.

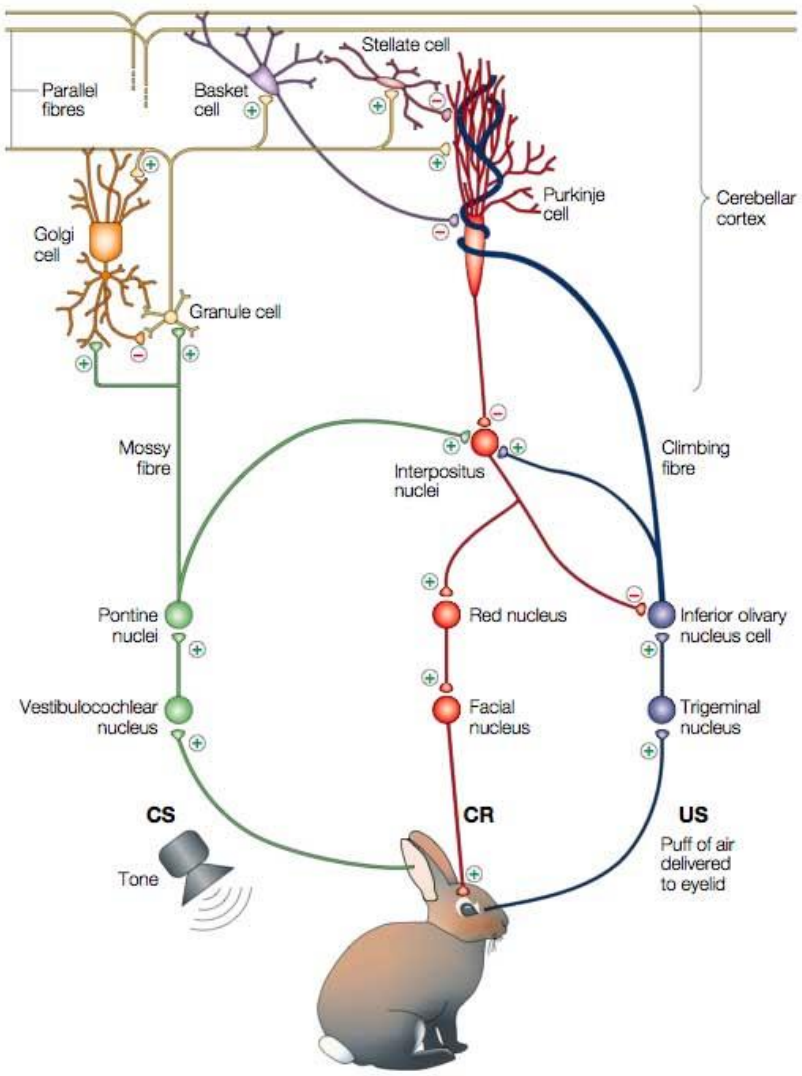


*Figure 20: Mechanism of learning in eye blinking*

The unconditioned stimulus (US), an air puff to the eyelid, automatically leads to a blink but also activates climbing fibers that originate in the inferior olive. Exactly one climbing fiber innervates one Purkinje neuron in the cerebellar cortex. This connection is powerful and results in very strong depolarization of the Purkinje cell. As stated above, activation of the Purkinje neuron results in the inhibition of the deep cerebellar nuclei.

In the figure 20 you can see the cerebellar mechanism of learning. From the anatomy of the cerebellum, it can be automatically realized that there are two sites of convergence for the US and CS pathways: the deep cerebellar nuclei and the Purkinje neuron.

### 5.2.1 Robotic implementation

In this protocol the Phantom Premium 1.0 placed in the vertical plane with three joint for it. Also the sinusoidal wave form as a desired position for the first joint was defined and for the second joint another trajectory was defined. However, for the third joint the desired position was fix and zero. Two tools is used here, one of them is attached to the end effector of the premium and another one is the target, both of them were observed by optical measurement system VICRA and recorded as an image.

In this protocol two methods were considered for the controller:

- Proportional controller (P)
- Proportional and derivative controller(PD)

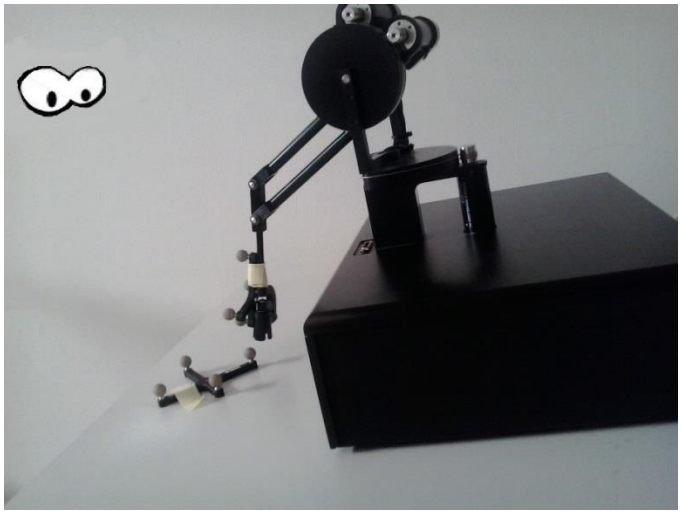

*Figure 21: premium robot in EBCC protocol*

### 5.2.2 Learning by Cerebellum Network with single Plasticity Site

In order to decrease the output error two methods were used, the proportional controller as the feedback controller and also the experimental PID tuning method for tuning the system.

Proportional Control is a useful method for designing control systems. In this control method, the control system acts in a way that the control effort is proportional to the error. In other words, the output of a proportional controller is the multiplication product of the error signal and the proportional gain. This can be mathematically expressed as: $P_{out} = K_p e(t) + P_0$

Where $P_0$ is Controller output with zero error, $P_{out}$ is Output of the proportional controller $K_p$ is Proportional gain , $e(t)$ is Instantaneous process error at time t, $e(t) = SP - PV$ where SP is Set point and PV is Process variable.

Currently, more than half of the controllers used in industry are PID controllers. In the past, many of these controllers were analog; however, many of today's controllers use digital signals and computers. When a mathematical model of a system is available, the parameters of the controller can

be explicitly determined. However, when a mathematical model is unavailable, the parameters must be determined experimentally. Controller tuning is the process of determining the controller parameters which produce the desired output. Controller tuning allows for optimization of a process and minimizes the error between the variable of the process and its set point.

Types of controller tuning methods include the trial and error method, and process reaction curve methods. The most common classical controller tuning methods are the Ziegler-Nichols and Cohen-Coon methods. These methods are often used when the mathematical model of the system is not available.

The trial and error tuning method is based on guess-and-check. In this method, the proportional action is the main control, while the integral and derivative actions refine it. The controller gain, Kc, is adjusted with the integral and derivative actions held at a minimum, until a desired output is obtained.

The time-evolving states were decoded into the granular layer. From granule cells, activity was transmitted to the PC and in parallel excited the DCN. The US-related pattern reached the Purkinje cell when US threshold was detected. The Purkinje cell in turn inhibited the DCN. At the beginning of the acquisition phase, Purkinje cell was spontaneously active, supplying tonic inhibition to the DCN (Fig. 22.A). After acquisition, PC activity was decreased; summing up all the presynaptic (constant or plastic) inputs to DCN, DCN neurons began to fire strongly before the onset of the US as neurorobot acquired the CR (Fig. 22.B).Then during extinction trials, PC activity was progressively re-increased; and DCN did not produce CR anymore (Fig. 22.C).

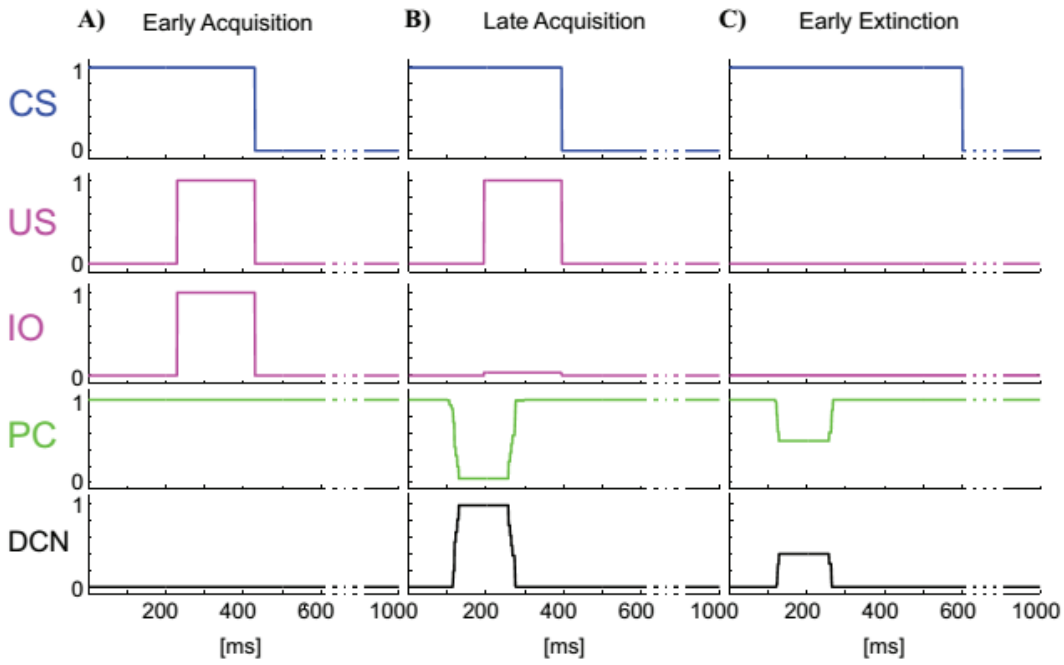


*Figure 22: Acquisition time*

The modulation of each plastic connection embedded into the cerebellar models represents the intrinsic mechanisms underlying these observed behaviors. For each trial, the PFs active without a correlated CF signal on the PC underwent an LTP, while PFs corresponding at the time-states when a signal arrived to the PC from CF developed LTD. Since the trial-by-trial variability within each test, the LTD/LTP did not develop perfectly in fixed PF-bundles; the most of PFs decoded system-state outside US (80% of trial duration) and thus maintained maximum values (saturated LTP); the PFs always decoding system-state during US underwent an equal strong LTD; the few PFs at the US time-window borders underwent different balance LTD/LTP, thus they spread within the weight ranges (0-1) (Fig.23.B, C, D, E).

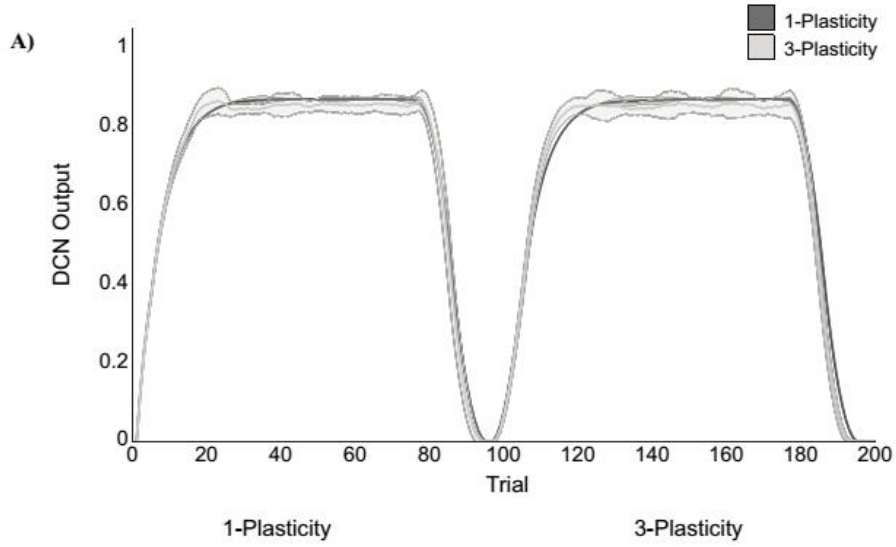

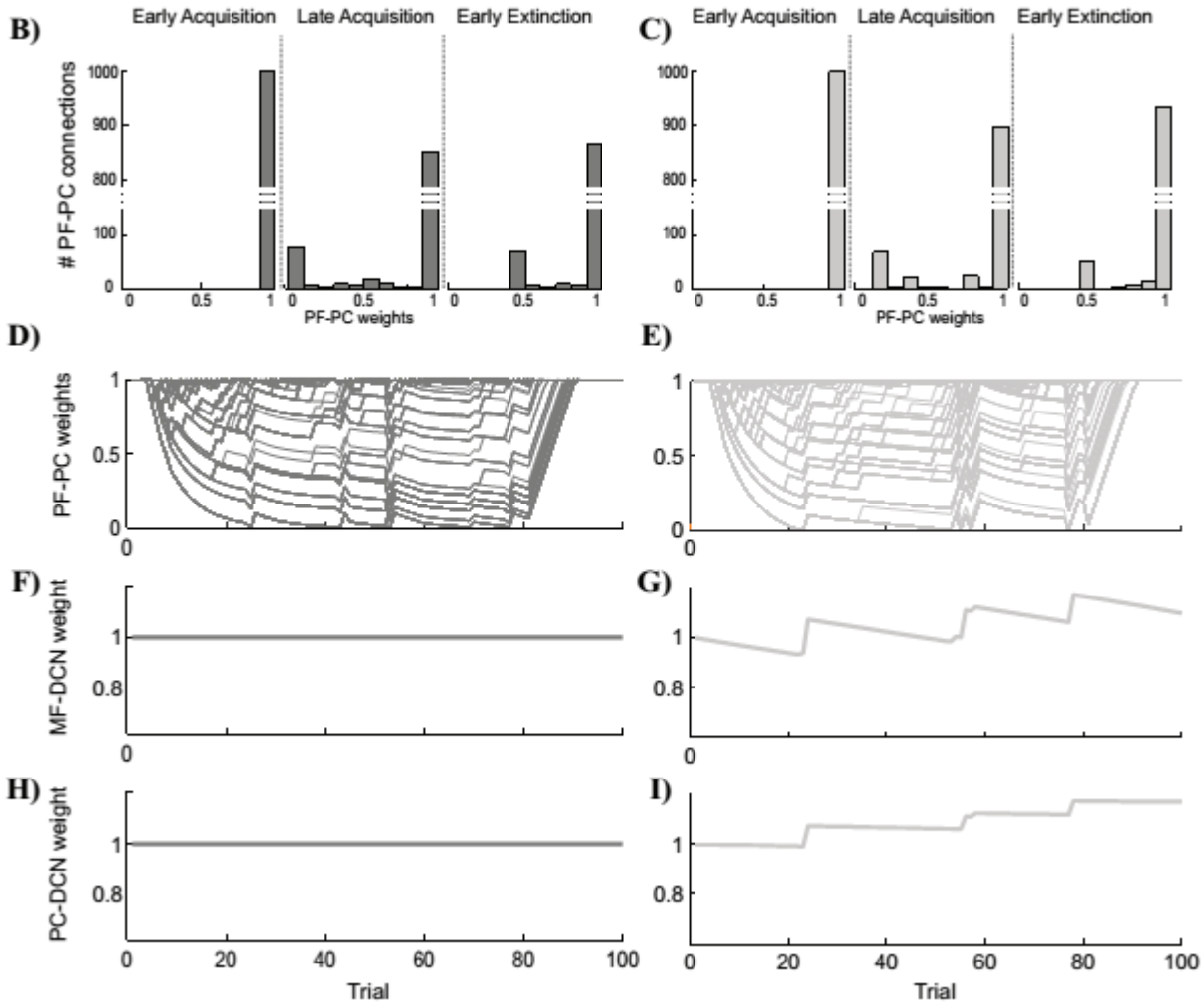


*Figure 23: Three plasticity weights and DCN output*

The main phenomenon driving acquisition was the development of LTD at the PF-PC synapses. In the 3-plasticity model, in the meanwhile, with a slower rate, plasticity at the MF-DCN synapse and at the PC–DCN synapse occurred (Fig. 23.F,G,H,I). Thus a partial transfer of activity generating motor response occurred from cortical to nuclear plasticity sites. In session1, this transfer did not change any overall learning performances. The network was able to rapidly extinct the stimuli association by fast PF-PC LTP, but without canceling the slower nuclear plastic changes had occurred. Thus, session2 controlled by the 3-plasticity model started with the cerebellar synapses in a different state than when controlled by the 1-plasticity model: the distributed plasticity dynamics, able to store information, was responsible for the higher learning rate in session2.

## 5.3 Multi-Rate Two State Model of Learning

The message is our results for both tasks reflect the Multi-rate adaptation processes as stated in the Multi-rate two state model of learning.

Savings is a fundamental property of memory. If savings is present, relearning will proceed more quickly than initial learning [37].

The study of Kojima showed that (1) savings can occur in a motor adaptation task, (2) it can cause a sudden jump in performance if a block of no-feedback (dark) trials is inserted between the extinction and re-adaptation blocks, and (3) it can be washed out if a block of baseline trials is inserted between the extinction and re-adaptation blocks.

We know that learning an initial motor adaptation reduces not only the initial performance but also the time constant for subsequently learning the opposite adaptation. Two other important observations are rapid DE- adaptation and rapid downscaling. Where fully or partially unlearning a motor adaptation can be faster than initial learning of this adaptation.

To account for the results of their savings experiments, Kojima et al. suggested a novel two-state model in which distinct mechanisms specialized in increasing the gain of saccades versus decreasing it. The two-state model in which each state learned at a different rate, rather than in a different direction, might be able to account for the full pattern of savings.

We simulated the progression of motor output in this learn unlearn-relearn paradigm a two-state, gain-independent, multi rate model. The learning rules for these models are shown below:

$$x_1(n+1) = A_f . x_1(n) + B_f . e(n)$$

$$x_2(n+1) = A_s . x_2(n) + B_s . e(n)$$

$$B_f > B_s , A_s > A_f$$

$$x = x_1 + x_2$$

X(n) is Net motor output on trial n, and X1 and X2 are internal states that contribute to the net motor output, e (n) is error on trial n, B is learning rate and A is Re-tension factor. In all these models error arises because there is a difference between the motor output x(n) and the state of the environment f(n) such that :e(n)=f(n)-x(n).

Our multi-rate model produce savings and predict decay in the amount of savings if null trials are inserted before the learning block as a figure 42:


*Figure 24: Paradigm for basic savings experiment.*

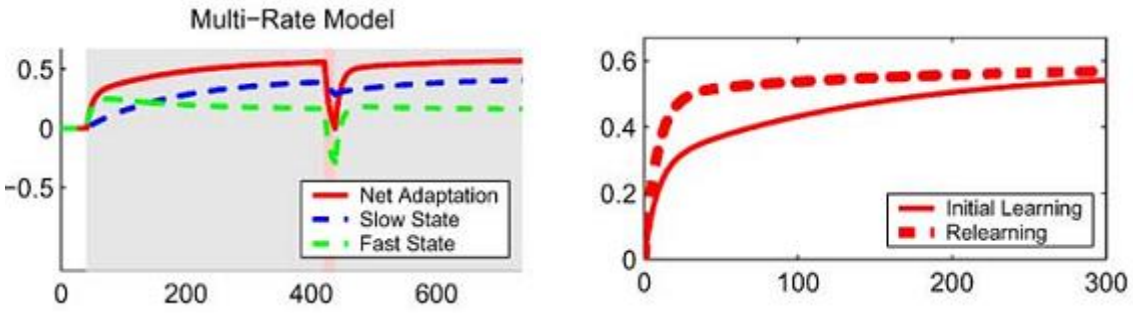


*Figure 25: Adaptation*

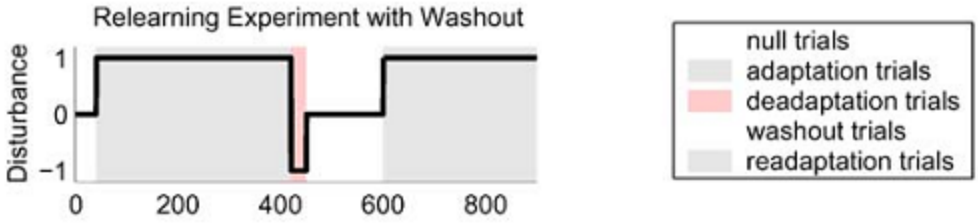


*Figure 26: Paradigm for savings experiment with washout*

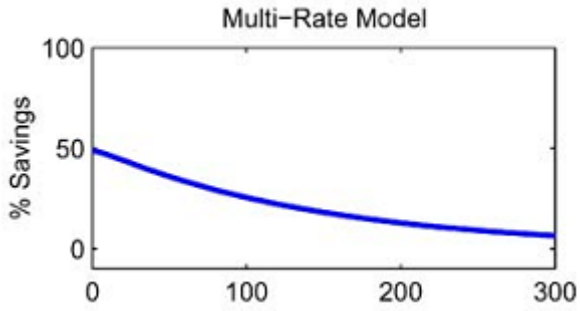


*Figure 27: The amount of savings found in simulation, as a function of the number of washout trials. The amount of savings is measured as the percent improvement in performance on the 30th trial in the relearning block compared to the 30th trial in the initial learning block.*

In the case of the multi-rate model, relearning is faster than initial learning because when relearning starts, the slow state is already biased towards relearning, making relearning more dependent on the fast state compared to initial learning.

The multi-rate model predicts a rebound effect, or spontaneous recovery, during this same period. Instead of remaining at zero, predicted motor output during the zero error block transiently rebounds toward the motor output during the initial learning block like the figure 28 (Error-clamp paradigm):

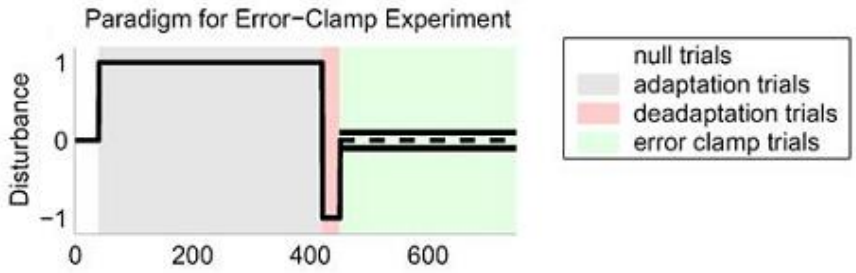


*Figure 28: Motor Adaptation in the Error-Clamp Paradigm*

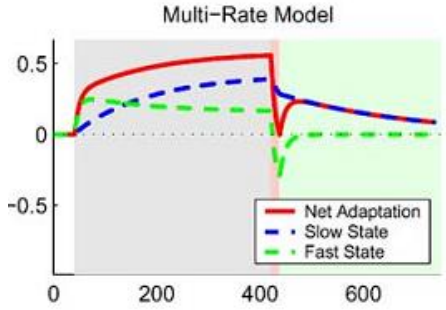


*Figure 29: the multi-rate model predicts a transient rebound of motor output in the error-clamp block. This rebound is in the direction of the motoroutput displayed in the initial learning block, resulting in spontaneous recovery.*

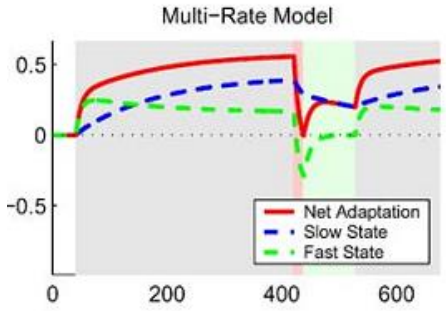


*Figure 30: The multi-rate model predicts that performance at the start of the relearning block is already better than baseline. This jump-up in performance is caused by adaptation rebound in the error-clamp phase*

The time course of the rebound—a rapid rise then a slow decline—was also predicted by the multi-rate model. Also in multi rate model the time constant for an initial motor adaptation is faster than the time constant for subsequent adaptation to the oppositely directed adaptation stimulus. The multi-rate model correctly predicts slower learning of the second adaptation in the interference paradigm. The multi-rate model predicts slower learning because the slow learning module is initially biased against learning the second adaptation.

The multi-rate model not only explains when a motor adaptation is learned then washed out, the rate of de-adaptation back to baseline can be faster than the rate of initial adaptation but explains why the apparent magnitude of this effect can vary substantially from one paradigm to another like the figure 31:

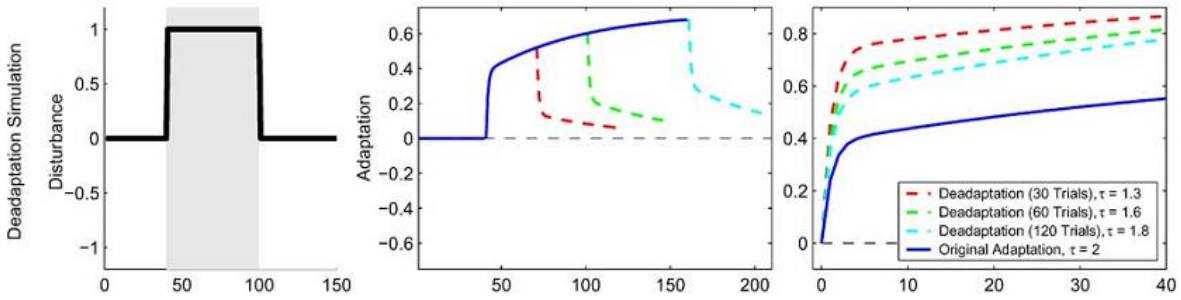


*Figure 31: Rapid unlearning*

Also the multi rate model can explain that the time constant for adapting to a scaled down version of a previously learned force-field adaptation can be even faster than the rate of de-adaptation to baseline. This effect can also be explained by the multi-rate model in Figure 32:

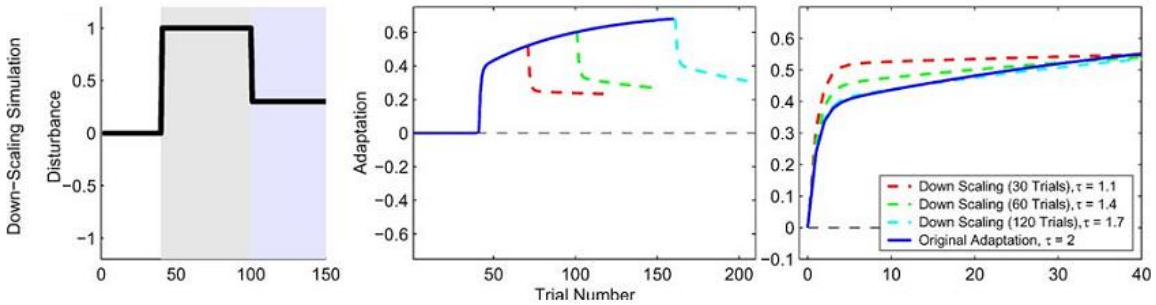


*Figure 32: Rapid downscaling*

One important feature of the class of multi rate model is that multiple realizations of the same input-output behavior are possible, i.e., internal system architectures are not unique. Of particular interest are the two equivalent system architectures diagrammed in Figure 33 and 34. In the first representation, two learning modules independently adapt from error and their outputs are combined to produce changes in net motor output. In the second representation, the two learning modules are cascaded such that the fast module adapts directly from error while the slow module adapts indirectly via the output of the fast module.

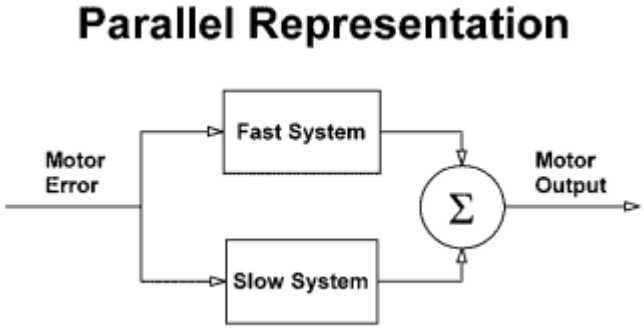


*Figure 33:* Two Different Internal Realizations of a Linear, *parallel representation*

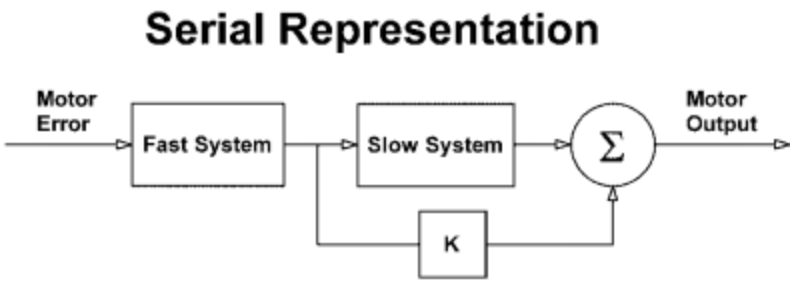


*Figure 34*: *Two Different Internal Realizations of a Linear, Two-State, and Multi-Rate System*

## 6. Discussion and Conclusions

In this work, two robotic protocols (Vestibulo-Ocular Reflex and Eyeblink Classical Conditioning) have been tested and implemented on a real robot and the embedded adaptive controller for cerebellum model has been developed. The main observation is that plastic mechanisms at DCN synapses effectively complement the learning capabilities of PF-PC synapses and contribute to the acquisition of the dynamics model of the arm or object plant. A correct synaptic weight adjust the DCN synapses that acts as a gain adaptation and allowing the PFs to work in their effective operative range, thus making the plasticity mechanisms between PFs and PCs more precise.

Two different learning time scales consisting of: (1) a fast learning process, in which temporal information was assumed and gathered from PF-PC synapses, and (2) a slow learning process, in which the cerebellar excitatory and inhibitory gain values were adapted in the DCN and the manipulation precision increased.

In this experiment, by ingratiating distributed synaptic plasticity and by generating closed-loop simulations, allowed to decrease the growing error based on feedback from the actual movement and accounted for three main theoretical point of cerebellar functioning.it means that (1) the cerebellum operates as a corrective inverse dynamic model. The granular layer was implemented as a non-periodic state generator. This states are then correlated with the error-based teaching signal received through the CFs [38]. (2) The PF-PC plasticity temporally connected the input state and the error estimation obtained during execution of the manipulation task. Instead, MF-DCN and PC-DCN plasticity's store the excitatory and inhibitory gain of the neural network required to generate accurate correction of movement. Thus, the DCN afferent synapses deduced the main properties of the object under manipulation, while the PF-PC synapses store the temporal characteristics of the task.(3) the evolution for the PF-PC plasticity is rapidly, while the evolution for the DCN plasticity is more slowly, because it depends on the previous evolution of plasticity at the PF-PC synapse itself.

According to what it said, this experiment proposes a reasonable describe on how multiple plasticity sites, including the PF-PC and the MF-DCN and PC-DCN synapses, may effectively implement cerebellar learning control.

The behavioral fall-outs of this model emerged in our tests. To our knowledge, it is the first time an embodied distributed realistic cerebellar model, tested in cerebellum-mediated paradigms, came

across able to robustly reproduce human-like effective learning properties in acquisition, extinction and re-acquisition, dealing with different external and noisy stimuli in real-world.

In the Pavlovian task, the neurorobot expressed response levels comparable to those found in human EBCC with similar ISIs, where a stable behavior was achieved in about 30 trials [39, 40]. Concerning the VOR task, neurophysiological studies showed how in a visual-vestibular training the cerebellum functioning led to an image slip minimization around 0.2° [41].

The 3-plasticity-site model unveiled in the motor memory transfer between cerebellar sites; in this way, the cerebellar model was equipped with the intrinsic capability to optimize the learning on multiple timescales and to effectively adapt to dynamic ranges of stimuli. These outcomes are consistent with the hypothesis about the coexistence of two processes proceeding at different rates in the cerebellum-mediated learning and located in different cerebellar sites, cerebellar cortex and deep cerebellar structures [42, 43].

In conclusion, we have linked low-level brain circuits with high-level functions integrating a detailed adaptive cerebellar controller into a neurorobot operating in real-time. The low-level embedded neuron connection dynamics were observed in high-level behavioral tasks: the fundamental aspects of cerebellar function - prediction, learning, timing and memory - were generated [44]. As a further advance, the platform could be updated with new neurophysiological properties and the distributed plasticity model could be translated into a more realistic spike-timing computational scheme [45].

In multi rate process cerebellar controller with multisite plasticity can effectively drive timing task as EBCC and complex VOR paradigm in a real robot. The multisite plasticity proved superior to single-site plasticity in generating human-like VOR acquisition, extinction and consolidation especially in complex tasks like gain-up and multi-session VOR.

The three plasticity controller was able to behave both as timing and gain controller, demonstrating high accuracy in a closed-loop sensorimotor task. The cerebellar model extension with the DCN plasticity sites improved robot adaptation allowing to deal with changing stimuli and environmental conditions.

## 7. References


[1] Chiel, H. J., & Beer, R. D. (1997). The brain has a body: adaptive behavior emerges from interactions of nervous system, body and environment. [Editorial Material]. Trends in Neurosciences, 20(12), 553-557.

[2] Fine EJ, Ionita CC, Lohr L (2002). "The history of the development of the cerebellar examination". Semin Neurol 22 (4): 375–84. Doi:10.1055/s-2002-36759.PMID 12539058.

[3] Albus, J. S. (1971). A theory of cerebellar function. Math. Biosci.10, 25–61.doi: 10.1016/0025-5564(71)90051-4.

[4] David Marr. A theory of cerebellar cortex. The Journal of physiology, 202(2):437–470, 1969.

[5] Wiener N: Cybernetics. J. Wiley; 1948.

[6] Sabes PN:The planning and control of reaching movements. Curr Opin eurobiol2000, 10:740-46

[7] N. Bernstein, The coordination and Regulation of Movements, Pergamon, London, 1967.

[8] P. Morasso, Spatial control of arm movements, Exp. Brain Res, 1981, Vol. 42, pp.223-227.

[9] T. Flash, N. Hogan, The co-ordination of arm movements: an experimentally confirmed mathematical model, J. Neurosci., 1985, Vol. 5, pp.1688-1703.

[10] Daniel M. Wolpert, R. Chris Miall and Mitsuo Kawato "Internal models in the cerebellum".

[11] Jeong Yoon Lee and Nicolas Schweighofer. Dual adaptation supports a parallel architecture of motor memory. The Journal of Neuroscience, 29(33):10396–10404, 2009.

[12] Reza Shadmehr, Maurice A Smith, and John W Krakauer. Error correction, sensory prediction, and adaptation in motor control. Annual review of neuroscience, 33:89–108, 2010.

[13] Maurice A Smith, Ali Ghazizadeh, and Reza Shadmehr. Interacting adaptive processes with different timescales underlie short-term motor learning. PLoS biology, 4(6):e179, 2006.

[14] Javier F Medina, Keith S Garcia, and Michael D Mauk. A mechanism for savings in the cerebellum.The Journal of Neuroscience, 21(11):4081–4089, 2001.

[15] Wei Zhang and David J Linden. Long-term depression at the mossy fiber–deep cerebellar nucleus synapse. The Journal of neuroscience, 26(26):6935–6944, 2006.

[16] J.F. Medina and M.D. Mauk. Computer simulation of cerebellar information processing. Nature Neuroscience, 3(SUPPL.):1205–1211, 2000.

[17] J.F. Medina, W.L. Nores, T. Ohyama, and M.D. Mauk. Mechanisms of cerebellar learning suggested by eyelid conditioning. Current Opinion in Neurobiology, 10(6):717–724, 2000.

[18] Vlastislav Bracha, Kristina B Irwin, Michelle L Webster, David A Wunderlich, Michal K Stachowiak, and James R Bloedel. Microinjections of anisomycin into the intermediate cerebellum during learning affect the acquisition of classically conditioned responses in the rabbit. Brain research, 788(1):169–178, 1998.

[19] Christopher Burdess. The vestibulo-ocular reflex: computation in the cerebellar flocculus. PhD thesis, Citeseer, 1996.

[20] Naoki Masuda and Shun-ichi Amari. A computational study of synaptic mechanisms of partial memory transfer in cerebellar vestibulo-ocular-reflex learning. Journal of computational neuroscience, 24(2):137–156, 2008.

[21] Philip JE Attwell, Shbana Rahman, and Christopher H Yeo. Acquisition of eyeblink conditioning is critically dependent on normal function in cerebellar cortical lobule hvi. The Journal of Neuroscience, 21(15):5715–5722, 2001.

[22] Phillip JE Attwell, Samuel F Cooke, and Christopher H Yeo. Cerebellar function in consolidation of a motor memory. Neuron, 34(6):1011–1020, 2002.

[23] John P Welsh and John A Harvey. Acute inactivation of the inferior olive blocks associative learning. European Journal of Neuroscience, 10(11):3321–3332, 1998.

[24] Chris I De Zeeuw and Christopher H Yeo. Time and tide in cerebellar memory formation. Current opinion in neurobiology, 15(6):667–674, 2005.

[25] Bazzigaluppi,P.,DeGruijl,J.R.,van der Giessen, R. S., Khosrovani, S.,DeZeeuw,C.I.,and deJeu,M.T.(2012). Olivary subthreshold oscillations and burst activity revisited.Front. Neural Circuits 6:91. doi:10.3389/fncir.2012.00091.

[26] Galliano, E., Gao, Z., Schonewille, M., Todorov, B., Simons, E., Pop,A. S., et al. (2013). Silencing the majority of cerebellar granule cells uncovers their essential role in motor learning and consolidation. Cell Rep.3, 1239–1251. doi: different studies have supported the existence of multiple forms of LTD10.1016/j.celrep.2013.03.023.

[27] Ito, M., and Kano, M. (1982). Longlasting depression of parallel fiberPurkinje cell transmission induced by conjunctive stimulation of parallel fibers and climbing fibers in the cerebellar cortex.Neurosci. Lett. 33, 253–258. doi: 10.1016/0304-3940(82)90380-9.

[28] Hansel, C., Linden, D. J., and Angelo, E. D. (2001). Beyond parallel fiber LTD: the diversity of synaptic and non-synaptic plasticity in the cerebellum.Nat. Neurosci.4, 467–476.

[29] Racine, R., Wilson, D.,Gingell, R., and Sunderland, D. (1986). Longterm potentiation in the interpositus and vestibular nuclei in the rat. Exp. Brain Res.63, 158–162. doi: 10.1007/BF00235658.

[30] Jesús A. Garrido, Niceto R. Luque, Egidio D'Angelo and Eduardo Ros "Distributed cerebellar plasticity implements adaptable gain control in a manipulation task: a closed-loop robotic simulation". doi: 10.3389/fncir.2013.00159

[31] Morishita, W., and Sastry, B. R. (1996). Postsynaptic mechanisms underlying long-term depression of GABAergic transmission in neurons of the deep cerebellar nuclei.J. Neurophysiol.76, 59–68.

[32] C. Burdess, The vestibulo-ocular reflex: computation in the cerebellar flocculus, 1996.

[33] M. Gerwig, F. P. Kolb, and D. Timmann, "The involvement of the human cerebellum in eyeblink conditioning," Cerebellum, vol. 6, no. 1, pp. 38–57, 2007.

[34] Claudia Casellato, Alberto Antonietti, Jesus Garrido, Richard Carrillo, Niceto R Luque, Eduardo Ros, Alessandra edrocchi, and Egidio D'Angelo. A generalized model of learning: robotic control driven by a spiking cerebellar network. Submitted to PlosOne

[35] Ito M (1982) Cerebellar control of the vestibulo-ocular reflex–around the flocculus hypothesis. Annual review of neuroscience 5: 275–297.

[36] D. S. Woodruff-Pak and J. E. Steinmetz, "Past, present, and future of human eyeblink classical conditioning," in Eyeblink Classical Conditioning: Volume I. Applications in Humans, Kluwer Academic, Norwell, Mass, USA, 2000.

[37] M. A. Smith, A. Ghazizadeh, and R. Shadmehr, "Interacting adaptive processes with different timescales underlie short-term motor learning," PLoS biology, vol. 4, no. 6, p. e179, 2006.

[38] Yamazaki, T., and Tanaka, S. (2005).Neural modeling of an internal clock. Neural Comput.17, 1032–1058. doi: 10.1162/0899766053491850.

[39] Vlastislav Bracha, Lingke Zhao, Kristina B Irwin, and James R Bloedel. The human cerebellum and associative learning: dissociation between the acquisition, retention and extinction of conditioned eyeblinks. Brain research, 860(1):87–94, 2000.

[40] Britt S Hoffland, Matteo Bologna, Panagiotis Kassavetis, James TH Teo, John C Rothwell, Christopher H Yeo, Bart P van de Warrenburg, and Mark J Edwards. Cerebellar theta burst stimulation impairs eyeblink classical conditioning. The Journal of physiology, 590(4):887–897, 2012.

[41] Rhea R Kimpo, Edward S Boyden, Akira Katoh, Michael C Ke, and Jennifer L Raymond. Distinct patterns of stimulus generalization of increases and decreases in vor gain. Journal of neurophysiology,94(5):3092–3100, 2005.

[42] Maurice A Smith, Ali Ghazizadeh, and Reza Shadmehr. Interacting adaptive processes with different timescales underlie short-term motor learning. PLoS biology, 4(6):e179,2006.

[43] Javier F Medina, Keith S Garcia, and Michael D Mauk. A mechanism for savings in the cerebellum.The Journal of Neuroscience, 21(11):4081–4089, 2001.

[44] Egidio D'Angelo, Sergio Solinas, Jesus Garrido, Claudia Casellato, Alessandra edrocchi, Jonathan Mapelli, Daniela Gandolfi, and Francesca Prestori. Realistic modeling of neurons and networks: towards brain simulation. Functional neurology, 28(3):153, 2013.

[45] Paul FMJ Verschure and Thomas Voegtlin. A bottom up approach towards the acquisition and expression of sequential representations applied to a behaving real-world device: Distributed adaptive control iii. Neural Networks, 11(7):1531–1549, 1998.